CALIFORNIA STATE UNIVERSITY, NORTHRIDGE

CHARACTERISTICS OF MIOCENE TO PLIOCENE SANDY UNITS IN THE HIKURANGI FOREARC, NORTH ISLAND, NEW ZEALAND

A thesis presented in partial fulfillment of the requirements

for the degree of Master of Science

in Geology

By

Kevin Scott Rivera

May 2010

The thesis of Kevin Scott Rivera is approved:

Jon R. Sloan, Ph.D.	Date
Vicki Pedone, Ph.D.	Date
Kathleen Marsaglia, Ph.D., Chair	Date

California State University, Northridge

ACKNOWLEDGMENTS

Funding for this project was provided by National Science Foundation grant (award # 0119936) in support of the Catalyst program at California State University, Northridge. I would like to thank my advisor Kathleen Marsaglia for all of her time, support and input in all phases of this project. I would also like to acknowledge Vicki Pedone who was instrumental in my decision to join the Catalyst Program and continue my education in the field of geological sciences. Field assistance was provided by former CSUN students Alyssa DeVaughn and Noelia Rodriguez. Michael Marden of Landcare Research NZ, Ltd. offered his resources to facilitate the completion of the field component of this study. I would finally like to thank my wife and family who always supported me, rarely complained about my strange hours, and always understood that my sometimes endless complaints about sandstone reflected my devotion to the topic.

TABLE OF CONTENTS

ABSTRACT

CHARACTERISTICS OF MIOCENE TO PLIOCENE SANDY UNITS IN THE HIKURANGI FOREARC, NORTH ISLAND, NEW ZEALAND

BY

Kevin Scott Rivera

Master of Science in Geology

This study was conducted to determine the petrographic characteristics, provenance, and reservoir potential of sandstone in the Wairoa syncline of North Island, New Zealand. Three intervals within the Middle Miocene to Pliocene section (Tolaga and Mangaheia Groups) were measured (total 420 m), described, and sampled at spacing ranging from 2 m to 20 m. These outcrops consist primarily of thinly to medium bedded, moderately hard to hard mudstone and fine-to medium-grained sandstone with minor fossiliferous sandstone and limestone. Cretaceous to Lower Miocene outcrops northwest of the section area were also described and sampled. Samples were thin-sectioned and impregnated with blue-dyed epoxy for porosity identification and sand-rich samples were stained for identification of calcium and potassium feldspar. Four hundred sand-sized grains in 33 stained thin sections were counted using the Gazzi-Dickinson method and divided into 19 mineral grain and lithic fragment compositional categories. Interstitial components, i.e. porosity, matrix, and cement, were also tallied. Sandstone samples vary from lithic to feldspathic graywackes and calcite-cemented litharenites to feldspathic litharenites (mean QFL 36: 29: 35; mean LmLvLs 27: 27: 46; mean QmKP 51: 13: 36). Porosity values range from <1.0% to 24.9% and average 6.4%.

Results from this study are consistent with those of previous workers who suggested that Miocene sedimentary successions in the Raukumara Peninsula were deposited along the slope in a forearc basin setting at bathyal depths whereas, the lower Pliocene units were most likely deposited on a shelf at shallower depths. Modal data for Miocene and Pliocene sandstones reflect the tectonic complexity of the region as the Hikurangi subduction margin evolved and suggest the most likely sediment sources were the Torlesse basement rocks in combination with volcanic input from the magmatic arc in the Northland-Coromandel region. Temporal trends in sandstone composition show a progressive increase in arc contribution throughout the Miocene followed by a decrease in the abundance of volcanic debris in the lower Pliocene possibly associated with the reorganization of the arc axis.

The major factors affecting overall porosity in Miocene to Pliocene sandstones from this study are total rock % carbonate cement, total rock % matrix and total rock % bioclasts. Higher percentages of any of these components are associated with lower overall visible porosity. Higher matrix percentage is linked to bioturbation, with thinner beds exhibiting higher degrees of bioturbation. Therefore, bed thickness and carbonate content are important factors in reservoir potential in these Miocene units. Carbonate cementation may be enhanced by the presence of bioclastic debris within the sandstone and the abundance of micritic carbonate within the surrounding mudstone.

INTRODUCTION

This study of sedimentary successions in the Raukumara Region of North Island, New Zealand (Fig. 1) was conducted to determine the petrology, provenance and reservoir characteristics of sandstone units that crop out in the area. Rock units included in the study are part of the Miocene Tolaga Group and Pliocene Mangaheia Group. The study included a field component consisting of the measurement and description of a series of stratigraphic sections as well as collection of outcrop samples and a laboratory component including sample preparation and petrographic analysis of representative sandstone samples. Results of this study are pertinent to ongoing studies of modern sand provenance associated with the nearby Waipoa MARGINS Source-to-Sink focus site (Carter et al., 2010) and potential petroleum exploration in the region (e.g., Davies et al., 2000).

Tectonic Setting

Located at the southern end of the Tonga-Kermadec-Hikurangi subduction zone (Field et al., 1997) (Fig. 1), New Zealand represents the land area of an otherwise largely submerged continental block that straddles the Australian and Pacific plate boundary. In the South Island of New Zealand, deformation associated with the subduction interface is transferred to the Alpine Transform Fault (Lamb, 1988; Reyners and Cowan, 1993). The North Island is characterized by westward subduction of Pacific Plate oceanic lithosphere beneath continental lithosphere of the Australian Plate at the Hikurangi Trough (Field et al., 1997).

The Hikurangi subduction zone comprises several tectonic elements (Field et al., 1997) including from west to east: 1) the Taupo volcanic zone, an ensialic extensional

basin that contains the present magmatic arc of the system (Cole, 1984), 2) the axial ranges, 3) the Hikurangi forearc, and 4) the Hikurangi subduction interface (Walcott, 1978; Cole and Lewis, 1981; van der Lingen, 1982; Kamp, 1988; Collot et al., 1996). The latter two elements are most pertinent to this study.

The Hikurangi forearc encompasses the area between the arc (Taupo volcanic zone) and the deformation front and comprises relatively uniform greywacke basement and a cover sequence of Cretaceous-Cenozoic sediments much of the way to the deformation front (Lewis and Pettinga, 1993). Lewis and Pettinga (1993) subdivided the forearc into three zones: 1) the predominantly onshore inner forearc; 2) the predominantly offshore imbricate frontal wedge (Fig. 1); and 3) a zone of frontal accretion. The area along the east coast of North Island, located along the boundary between the inner forearc and the imbricate frontal wedge, is a zone of rapid uplift forming the coastal ranges. This zone is commonly referred to as the highest accretionary ridge or outer arc high (Cole and Lewis, 1981; Pettinga, 1982; Berryman et al., 1989). The inner forearc is synonymous with forearc basin. Field et al. (1997) prefer this term as the inner forearc is presently elevated above sea level and is therefore no longer accumulating marine sediments (excluding Hawke Bay embayment). Widespread active deformation occurs in the inner forearc with varying degrees of type and intensity. In the Raukumara area, high uplift rates and extensive normal faulting occur (Yoshikawa et al., 1980; Mazengarb, 1982 and 1984; Thornley, 1996). The least deformed area is a strip along the eastern side of the axial ranges through Hawke Bay, gradually widening north to include the Wairoa Syncline (Field et al., 1997) (Figs. 1 and 2). Marine sediments accumulated here throughout Miocene-Pliocene time in a typical forearc basin

setting (Cole and Lewis, 1981; van der Lingen, 1982), but deposition ceased in the late Pliocene through early Pleistocene.

Geology and Tectonic History

As described by Mazengarb and Speeden (2000), the rocks of the Raukumara area are subdivided into five major subunits based predominately on their age and structural history: 1) Upper Jurassic and Lower Cretaceous metasedimentary basement; 2) in-place Cretaceous to Oligocene sedimentary rocks; 3) the East Coast Allochthon (Lower Cretaceous to Oligocene displaced sedimentary rocks); 4) Miocene and Pliocene sedimentary rocks; 5) and Quaternary sediments (Fig. 2).

Within the Raukumara area, the Upper Jurassic to Lower Cretaceous basement rocks are part of the Torlesse composite terrane (Coombs et al., 1976; Bishop et al., 1985; Bradshaw, 1993) that formed as an accretionary prism at a convergent margin on the edge of the Gondwana supercontinent (Bishop et al., 1985; Adams and Kelley, 1998). In the study area they are part of the Pahau subterrane (that include the Waioeka and Omaio petrofacies) of Mortimer (1995), which consist of low-grade metasedimentary (deep marine mudstone and sandstone) rocks that form the axial ranges of the Raukumara region in North Island, New Zealand (Mazengarb and Speden, 2000).

Upper Cretaceous rocks that overly the Waioeka and Omaio petrofacies in the Raukumara area (Fig. 2) were deposited during the transition from a subduction to a passive margin at the end of the Mesozoic (Ballance, 1976). The Matawai Group comprises sedimentary formations of Early to Late Cretaceous age. Stratigraphy varies within the unit and consists of fine to coarse-grained sandstone, fossiliferous sandstone, conglomerate, breccia, mudstone, and tuff beds. Lateral facies changes within the

Matawai Group suggest a west to east transition from shelf to bathyal sequences (Mazengarb and Speden, 2000).

Matawai Group rocks are overlain in the west and northeast of the Raukumara region by the Tinui Group (Moore et al., 1986). A predominantly mudstone unit, the Tinui Group is latest Cretaceous to Paleocene in age and was deposited during folding, uplift and erosion of the Matawai Group rocks. Conformably overlying the basal Tinui Group sandstone facies is the thick, mudstone rich, geographically widespread Whangai Formation consisting of up to 500 m of noncalcareous and calcareous shale and mudstone (Mazengarb and Speden, 2000). The Whangai Formation is in conformable and gradational contact with the overlying Waipawa Formation (a.k.a. Waipawa Black Shale). This unit of dark gray to black, noncalcareous, micaceous mudstone is Late Paleocene in age with foraminifera indicative of deposition in outer shelf to upper bathyal water depths (Field et al., 1997). Typical samples of the shale have 2 - 6% TOC (total organic carbon) and the unit has by far the highest hydrocarbon-generating potential of any source rock on the east coast of North Island (Field et al., 1997).

Rocks of Eocene to Oligocene age (Mangatu Group) overly the Upper Cretaceous to Paleocene units. The Mangatu Group includes the Wanstead Formation, a 200-m-thick unit of alternating sandstone and blue-gray, calcareous, glauconitic mudstone that conformably overlies the Waipawa Formation. The Wanstead Formation is in turn, unconformably overlain by the 400-meter-thick, glauconitic sandstone and mudstone of the Weber Formation. Foraminifera from both formations suggest deposition was mainly at mid-bathyal depths (Mazengarb and Speeden, 2000).

During the Early Miocene a major change in tectonic setting occurred as a result of the reactivation and propagation of a subduction plate boundary through the region. Emplacement of the East Coast Allochthon (Fig. 2) occurred owing to SSW-directed subduction of the Pacific plate beneath the continental margin (Mazengarb and Speden, 2000). Deeper marine Upper Cretaceous to Oligocene passive margin sequences were uplifted, dissected and emplaced over their autochthonous shallower equivalents along a series of thrust sheets forming the East Coast Allochthon. A sedimentary sequence of Miocene to Pliocene age (Tolaga and Mangaheia Groups) unconformably overlies both the in-place Lower Cretaceous to Oligocene sequence and the East Coast Allochthon. This unconformity represents a major change in depositional environment associated with the inception of subduction (Ballance, 1976; Pettinga, 1982; Rait et al., 1991).

As obduction ceased in the Early Miocene, subduction related deformation and volcanism continued through the Middle and Late Miocene during which a series of folds and faulted antiformal structures developed (Mazengarb and Speden, 2000). Differential uplift and subsidence continued throughout the Late Miocene resulting in the formation of a structural high in the area now known as the Mahia Peninsula (Fig. 2). West of this high, within the subsiding Wairoa Basin, thick sequences of sediments were deposited into the Pliocene (Mazengarb and Speden, 2000).

Much of the Raukumara area has probably been emergent since the middle Pliocene (Mazengarb and Speeden, 2000). Uplift rates for the region vary between 1-4 mm/yr from the late Pleistocene to Holocene time period (Berryman, 1993; Ota et al., 1992). Yoshikawa (1988) suggests the Raukumara Peninsula is currently being upwarped asymmetrically as a growing anticlinal structure.

Miocene and Pliocene Rocks of the Wairoa Region

Miocene to Pliocene rocks of the Wairoa Region are subdivided into the Tolaga Group (Lower to Upper Miocene) and the unconformably overlying Mangaheia Group (uppermost Miocene to lower Pliocene) as described by Mazengarb et al. (1991).

Lower Miocene rocks of the Tolaga Group consist predominantly of massive and thinly bedded mudstones that are moderately hard, gray, and slightly calcareous, with interbeds of fine-grained sandstone and tuff (Mazengarb and Speeden, 2000). Macrofossils are rare within the unit whereas microfossils (mostly foraminifera) are common. Bedding thickness varies from millimeter-laminated mudstone to centimeter to meter-bedded sandstone and mudstone. There is considerable variation in both thickness and facies of the Lower Miocene rocks within the Raukumara area.

Middle Miocene rocks of the Tolaga Group unconformably overlie Lower Miocene rocks and typically consist of alternating, centimeter to decimeter-bedded, fine-grained sandstone and mudstone. Within the study area, Tolaga Group rocks of the Tunanui Formation are up to 2000 m thick (Field et al., 1997) whereas in northern Hawke Bay (south of the study area) similar units of alternating mudstone and sandstone have been mapped as the Makeretu or Rerepe sandstone of late Middle Miocene age (Mazengarb and Speeden, 2000).

Conformably overlying the Middle Miocene rocks are similar rocks of Upper Miocene age that consist of predominantly mudstone and alternating mudstone with interbedded sandstone. Between Gisborne and Wairoa (Fig. 2) these units have been mapped as the Makaretu Sandstone (Davies et al., 1998). Northwest of Wairoa, the

Makaretu Sandstone ranges up to 400 m thick and is interpreted as a lower bathyal sequence comprising four principal turbidite lobes (Davies et al., 2000).

The uppermost Miocene to Pliocene Mangaheia Group consists of up to 2000 m of shelly sandstone, sandstone and mudstone (Mazengarb and Speeden, 2000). Near the study area (Fig. 2) the unit consists mainly of sandstone and mudstone with several unconformable, discontinuous, shelly limestone intervals such as the Opoiti Limestone, which grades laterally into sandstone on both limbs of the Wairoa Syncline (Beu, 1995).

In his study of silicic tuffs in the Miocene and Pliocene marine successions of both North and South Island, New Zealand, Gosson (1986) determined the chronology of silicic volcanism and clarified the tectonic setting of the volcanic source centers and basins in which the ash was deposited. Thirty stratigraphic sections were measured and described throughout North and South Island, one of which (Hangaroa River Section) encompasses the three sections measured in more detail by this study (Figs. 3 and 4).

Study Area Location and Physiography

The study area is located in the southern region of the Raukumara Peninsula, the easternmost part of North Island, New Zealand (Figs. 1 and 2). The Raukumara area encompasses several distinct geomorphic regions including the Raukumara Range and the area between the Raukumara Range and the coast (eastern foreland) (Mazengarb and Speeden, 2000).

The Raukumara Range represents the northeast extension of the North Island axial ranges. The mountain belt is over 35 km wide and has maximum topographic relief of 1752 m. Predominantly covered in native forest, the topography is typically steep with

deeply incised drainages (gorges) although gently dipping, elevated surfaces top many peaks (Mazengarb and Speeden, 2000).

The eastern foreland geomorphic province (Fig. 1) encompasses the areas east and south of the Raukumara Range. The majority of the foreland is less than 1000 meters in elevation and consists of various landforms owing to the dynamic underlying geology. Several major river catchments (e.g., Waipaoa and Wairoa) (Fig. 2) are located within the foreland and extend to the flank of the Raukumara Range leading to deeply incised topography within those drainages. Extensive hillside erosion, landsliding and stream aggradation is prevalent in the area and terrace development is widespread in many of the catchments (Mazengarb and Speeden, 2000).

Situated within the eastern foreland and located inside the Wairoa catchment, the study area (Figs. 1 and 2) is approximately 35 km west of the city of Gisborne along state highway 36 (a.k.a. Tiniroto Road). Measured section locations for this study consist of roadside exposures along the eastern banks of the Hangaroa River and Mangawehi Stream, both tributaries to the Wairoa River. Topography within the study area varies between hummocky, rolling terrain to deeply incised drainages leading to steep, ridge and valley landforms. Maximum topographic relief within the area is approximately 420 meters.

METHODS

Three stratigraphic intervals of Middle Miocene to Pliocene sedimentary rocks within an approximately 2100-m-thick, partially exposed sedimentary succession along the Hangaroa River and Mangawehi Stream were measured, described and sampled in June of 2003 (Figs. 3, 4 and 5A-C). These units are part of the undifferentiated Miocene Tolaga Group and Pliocene Mangaheia Group. Locations for measured intervals were based primarily on exposure and accessibility to roadcuts along state highway 36 (a.k.a. Tiniroto Road). Although better exposures of sedimentary successions exist within the Hangaroa riverbed, high stream-flow levels at the time of fieldwork required the use of roadcuts for this study. Measurements were made using Jacob-Staff and tape-and-compass methods. The intervals, identified as Sections A, B and C, have a combined thickness of 420 m (Figs. 4 and 5A-C). Description of the measured sections included field observations that determined lithology, color (Rock-Color Chart Committee, 1991), bedding thickness, sedimentary structures, grain-size and sorting.

A total of sixty samples were collected within Middle Miocene to Pliocene measured sections locations at intervals between 2 and 10 meters: 11 from section A, 23 from section B, and 26 from section C. Ten outcrop samples from isolated exposures between sections were also collected. Additionally, eight samples from Cretaceous to Lower Miocene sedimentary outcrops were obtained from roadcuts northwest of the study area (Fig. 2).

Thin sections were prepared from outcrop samples after they were trimmed, cut into billets and impregnated with blue-dyed epoxy for porosity identification. These were reviewed and described for lithology. The Udden-Wentworth scale (Wentworth, 1922)

was used to differentiate between sand, silt and clay sized grains and the general term mudstone is used for clay and silt-rich rocks. Rocks were named using the classification schemes of Folk et al. (1970; sandstone) and Dunham (1962; carbonate). Many mudstone samples probably contain enough micritic carbonate to be termed calcareous mudstones or marlstones.

Selected thin-sections containing significant siliciclastic sand-sized fractions were then stained to differentiate between sodium and potassium feldspar. The staining process, described in Marsaglia and Tazaki (1992), consists of etching the thin section with concentrated hydrofluoric acid then staining with barium chloride, sodium cobaltinitrate and amaranth solutions.

Detrital modes of 33 selected thin sections were determined petrographically using an automated-stage point-counting system and a Nikon Eclipse E600 Pol research microscope. To minimize dependency of composition on grain size, the Gazzi-Dickinson method was used (Ingersoll et al., 1984). Four-hundred sand grains in each thin section were counted. Grid spacing larger than the maximum grain size was used to avoid multiple counting of individual grains. Counted grains were divided into 19 mineral grain and lithic fragment compositional categories (Tables 1 and 2). Interstitial components were also tallied (i.e. porosity, matrix, and cement) and are included in Tables 1 and 2. Total points counted (grains and interstitial) per thin section ranged from 478 to 916. Recalculated parameters are defined in Table 2 and were determined using a Microsoft Excel spreadsheet program.

RESULTS

Measured Stratigraphic Sections

Section A (Fig. 5A), a Middle Miocene road-cut exposure along the Mangawehi Stream, has a total thickness of 110 meters. Outcrop within this interval consists of moderately to steeply dipping (48° – 75°), thinly to moderately-bedded (cm-dm), moderately resistant gray mudstone, and resistant, fine-grained sandstone with scattered calcareous nodules and concretions (Fig. 6 A and B). Bedding contacts range from gradational to sharp. Sedimentary structures, other than discrete burrows, are absent owing to intense bioturbation throughout the section. Eleven outcrop samples were collected within this section at approximately 10-m intervals (Fig. 5A). Of the eleven samples collected from Section A, four consist of fine-grained sandstone whereas the remaining seven are mudstone. In thin section, sandstone samples are fine-grained, texturally immature, well to moderately sorted, calcite-cemented, feldspathic litharenites and lithic arkoses with angular to subrounded grains (Fig. 7). Bioclastic debris and volcanic lithic fragments are common in the sandstone. Other lithologies samples consist of gray-brown mudstone comprising varying proportions of clay and silt-sized particles, the latter being quartz with lesser feldspar and lithic fragments (Fig. 8 A and B). Bioclastic debris is common in the mudstone including mollusk and foraminifera fragments with lesser calcareous sponge spicules and agglutinated formanifera. Micritic carbonate is a rare to common matrix component. Glauconite pellets are present within all mudstone samples.

Section B (Fig. 5B), an Upper Miocene road-cut exposure along the Hangaroa River, has a total thickness of 185 meters. Outcrop within this interval consists of

moderately dipping (42° - 55°), thinly to moderately bedded (cm-dm), moderately resistant gray mudstone, and resistant, fine-grained sandstone with scattered calcareous nodules and concretions (Fig. 6 C and D). Bedding contacts range from gradational to sharp. Sedimentary structures, other than discrete burrows, are absent owing to intense bioturbation throughout the section. Twenty-three outcrop samples were collected within this section at approximately 10 to 20 m intervals with a few sampling intervals between 0.25 and 1 m. Of the 23 samples collected from Section B, ten are fine- to medium-grained sandstone, whereas the remaining samples are mudstone. In thin section, sandstone samples are fine to medium-grained, texturally immature, well to moderately sorted, calcite-cemented feldspathic litharenites to lithic graywackes with angular to subrounded grains (Fig. 9). Bioclastic debris and volcanic lithic fragments are common in the sandstone. Other lithologies consist of gray-brown mudstone comprising varying proportions of clay and silt-sized particles, including quartz with lesser feldspar and lithic fragments (Fig. 8 C and D). Bioclastic debris is common in the mudstone including mollusk and foraminifera fragments with lesser calcareous sponge spicules and agglutinated formanifera. Micritic carbonate is a rare to common matrix component. Glauconite pellets are present within all mudstone samples.

Section C (Fig. 5C), an Upper Miocene to Lower Pliocene road-cut exposure along the Hangaroa River, has a total thickness of 125 m. Of the 26 outcrop samples collected within this section at approximately 2 to 10 m intervals, nine consist of fine- to medium-grained sandstone whereas the remaining samples consist of fossiliferous packstone (2) or mudstone (15). Outcrop within the lower part of measured section C (Upper Miocene interval, 0-70 m) consists of moderately dipping (18° - 26°), thinly to

moderately-bedded (cm-dm), moderately resistant gray mudstone and resistant, fine-grained sandstone (Fig. 6 E). Bedding contacts range from gradational to sharp. Sedimentary structures, other than discrete burrows, are absent owing to intense bioturbation throughout the section. Unconformably overlying the Upper Miocene sequence, the Pliocene interval (70-125 m) consists of light olive-gray, resistant, coarse-grained, fossiliferous wackestone (70-73 m), dark olive-gray, resistant, fossiliferous packstone (73-90 m) and light olive-gray to yellowish-orange, moderately resistant, thinly-bedded, fine- to medium-grained sandstone with scattered calcareous nodules and concretions and interbedded with moderately resistant mudstone (90-125 m) (Fig. 5C). In thin section, sandstone samples from Section C are fine to medium-grained, texturally immature, well to moderately sorted, calcite cemented feldspathic litharenites to lithic graywackes with angular to subrounded grains (Fig. 10). Bioclastic debris and volcanic lithic fragments are common in many of the sandstone samples. Mudstone samples are gray brown and comprise varying percentages clay and silt sized particles, including quartz with lesser feldspar and lithic fragments. Bioclastic debris is common in mudstone samples including mollusk and foraminifera fragments with lesser sponge spicules and agglutinated formanifera. Micritic carbonate is a rare to common matrix component (Fig. 8 E and F). Glauconite pellets are present in all mudstone samples and most sandstone samples. Packstone samples are calcite-cemented, coarse-grained, poorly sorted with angular to sub-rounded grains, and abundant bioclastic debris including mollusk and foraminifera fragments with lesser sponge spicules and red algae fragments (Fig. 11).

Additionally, ten samples were collected at various locations between Sections A, B and C where exposed bedrock was accessible. Two Middle Miocene samples collected between Sections A and B were taken from beds of fine-grained sandstone with scattered calcareous nodules and concretions (samples HAB1 and HAB2). The other eight Middle and Upper Miocene samples taken from locations between Sections A, B and C are mudstone. All ten sandstone and mudstone samples are petrographically similar to the facies that over and underlie them as described above and below.

Other Samples

Cretaceous to Lower Miocene samples were collected from outcrop exposures northwest of the measured section locations (Fig. 2).

Two Cretaceous samples were collected from a roadside exposure. The outcrop consists of massive, moderately resistant gray mudstone and lesser fine-grained sandstone. Bedding contacts in outcrop are gradational and no sedimentary structures were observed. In thin section the sandstone sample (NZ-03-211) is a fine-grained, texturally immature, moderately sorted, feldspathic graywacke with angular to subrounded grains. Bioclastic debris and volcanic lithic fragments are rare within the sample. The other sample consists of gray mudstone comprising varying proportions of clay and silt-sized particles, including quartz with lesser feldspar and lithic fragments. Micritic carbonate is absent in this sample.

One Oligocene and one Paleocene sample were collected from massive, moderately resistant, gray mudstone outcrops northwest of the study area. Both samples are mudstone with varying proportions of clay and silt-sized particles, including quartz

with lesser feldspar and lithic fragments. Bioclasts, volcanic lithic fragments, bioclastic debris and micritic carbonate are absent in both samples.

Eight Lower Miocene samples were collected at various locations northwest of the study area (Fig. 2). Outcrops consisted of predominantly massive, moderately resistant gray mudstone and fine-grained sandstone. Bedding contacts are gradational at all locations and sedimentary structures, other than discrete burrows, were absent owing to intense bioturbation throughout the units. Six of the eight samples are fine- to medium-grained sandstone (NZ03-201, 202, 203, 204, 206, 212) and the remaining two are mudstone. In thin section, sandstone samples are fine to medium-grained, texturally immature, well to moderately sorted, calcite-cemented feldspathic litharenites to lithic graywackes with angular to subrounded grains. Bioclastic debris and volcanic lithic fragments are rare to common in the sandstone samples. The other two samples consist of gray-brown mudstone comprising varying percentages clay and silt sized particles, including quartz with lesser feldspar and lithic fragments. Bioclastic debris is common in the mudstone samples including mollusk and foraminifera fragments with lesser sponge spicules and agglutinated formanifera. Micritic carbonate is a rare to common matrix component.

Sandstone Petrography

The 33 sandstone samples petrographically analyzed for this study are composed of varying percentages of sand-sized quartz, feldspar and lithic fragments (Tables 1 and 2). Monomineralic sand components consist mostly of quartz, with lesser feldspar. Quartz grains exhibit straight to undulose extinction and are observed primarily as individual monocrystaline grains with lesser occurrences as sand-sized components of

sedimentary lithic fragments. Polycrystalline quartz, including chert, accounts for less than 7% of the framework grains. Plagioclase feldspar is common in all samples occurring mostly as individual monocrystaline grains and, to a lesser extent, as sand-sized components of sedimentary lithic fragments. Although many plagioclase grains are fresh, a significant number exhibit varying degrees of alteration to sericite and kaolinite. Additionally, plagioclase dissolution is common in several samples. Potassium feldspar is also present in all samples (but to a lesser degree than plagioclase) and occurs predominately as individual monocrystalline grains. Other rare components identified in several samples include biotite (fresh and altered), muscovite, chlorite, and dense minerals including zircon, sphene and tourmaline. Glauconite pellets are present in varying percentages in all but two samples.

On average, lithic fragments are predominately sedimentary and consist of mostly mudstone/shale, with lesser siltstone and rare carbonate and chert fragments. Metamorphic lithic fragments are dominated by quartz-mica tectonite with rare quartz-mica-feldspar aggregate. Volcanic lithic fragments consist of varying percentages of altered to unaltered fragments exhibiting microlitic, vitric, and felsitic textures. Although fresh volcanic glass is rare to absent in most samples, a few contain up to 50% unaltered volcanic glass in overall lithic content and one sample (tuffaceous sandstone) has up to 91%.

Bioclastic material is present in all but one sample (Cretaceous) in varying percentages. Bioclasts are predominately foraminifera and molluska fragments with lesser calcareous sponge spicules, diatoms and red algae fragments.

All but four samples contain matrix. Total rock percent matrix ranges from <1.0 to 43.0% with an average of 12.5%.

Equant carbonate is the main cementing agent and occurs in 25 of the 33 sandstone samples. The majority of carbonate cement fills interparticle pore space but numerous samples exhibit carbonate cementation within intraparticle pore space within feldspars (secondary) and bioclasts (primary and secondary) that have been partly to wholly dissolved. Clay-rim cements are generally very minor to absent (Tables 1 and 2), except in sample HA11. Total rock percent cement varies between <1 and 28% and averages approximately 12%. General cement related trends show a decrease in total percent porosity and matrix with increase in cement percentage although few samples contain appreciable amounts (>10%) of both cement and matrix.

Sandstone Porosity

The one Cretaceous sandstone sample analyzed in this study has less than 1.0 % porosity. It is not cemented and is a matrix-rich (43%) fine-grained, moderately to poorly sorted, feldspathic wacke with subrounded to subangular grains. Grain contacts range between point, long and concavo-convex.

Porosity values from Lower Miocene samples range between <1.0 and 10.2% with an average of 5.3%. IGV (intergranular volume = intergranular porespace + intergranular cement) in these samples ranges between 7.1 and 22.8% with an average of 11.3%. Of the six samples observed, the two most porous (NZ-03-201 and -202) are from thinly bedded, fine-grained, moderately sorted sandstone beds with angular to sub-rounded grains. Dominant porosity in these two samples is of primary, intergranular origin. Variable features affecting porosity are present within the two porous samples.

Sample NZ-03-201 (10.0 % porosity) is calcite-cemented and moderately compacted (long and concavo-convex grain contacts) with compacted sedimentary lithics reducing pore space. In contrast, sample NZ-03-202 (10.2% porosity) contains no calcite cement, has floating and point grain contacts but contains greater than 20% clay matrix.

Porosity values from the Middle Miocene samples from Section A range between <1.4 – 9.0% with an average of 4.9% (Fig. 7). IGV values in these samples range between 2.6 and 29.9% with an average of 20.3%. Sandstones within this section are typically thinly bedded (cm-dm), fine-grained, moderately to poorly sorted and tightly cemented with angular to subrounded grains. There are no moderately porous (> 10.0%) samples in this unit.

Porosity values from the Upper Miocene samples in sections B and C range between 0.0 and 24.9% with an average of 7.2% (Figs. 9 and 10). IGV values range between 6.9 and 29.5% with an average of 17.8%. Of the twelve Upper Miocene samples collected, four are moderately porous (> 10%). Three of the samples (NZ-03-HB1: 11.5%, NZ-03-HB12: 18.6%, NZ-03-HB20: 20.3%) are thinly-bedded (cm-dm), fine- to medium-grained, poorly to moderately sorted, lithic arenites with subangular to subrounded grains. Each of these samples contains less than 9% cement and/or matrix. Grain contacts are typically point, long and concavo-convex and each sample has minor compacted sedimentary lithics reducing pore space. Porosity within these samples is predominately intergranular and primary in nature although each displays minor intragranular porosity within foraminifera. This intragranular porosity accounts for 15% or less of total porosity within samples. The fourth porous sample (NZ-03-HC1: 24.9%) in this group is a volcanic lithic graywacke (tuffaceous sandstone) and is composed of

predominately unaltered, vesicular volcanic glass with lesser coarse-grained plagioclase and rare quartz. The sample is contains no cement but has appreciable clay matrix (17.5%). There are subequal amounts of intergranular and intragranular porosity owing to the extremely porous nature of the pumiceous volcanic glass components.

Pliocene sandstone samples from Section C range from arkosic arenites to lithic graywackes. Of the nine Pliocene sandstone samples from Section C, eight have porosity values that range from <1.0 to 9.0% with an average of 3.2% and are tightly cemented or matrix rich (Fig. 10). IGV values for these samples range between 1.9 and 21.4% and have an average of 11.8%. The ninth sample (NZ-03-HC1) has a porosity value of 24.4% and is a medium to coarse-grained, volcanic lithic arenite. Detrital grains within this sample are subangular to subrounded and poorly sorted with point, long and concavo-convex contacts. Minor dissolution occurs in both bioclastic debris and plagioclase grains but accounts for less than 2% of the overall porosity. The majority of primary porosity is intergranular although, owing to the porous nature of the vesicular volcanic glass, intragranular porosity within this sample is 24% of total rock percent porosity.

Sandstone Detrital Modes

The sandstone detrital modes are plotted on various ternary diagrams in Figure 12. Except for a few outliers, the samples cluster on the QFL and QmKP ternary plots and show the most variation in terms of lithic composition (LmLvLs). Overall, the Cretaceous sample is the most quartzose and contains the least amount of volcanic lithics (Fig. 12). Mean trends from the Cretaceous through Miocene time interval show sub-linear increases in QFL%L, LmLvLs%Lv and QmKP%P with corresponding sub-linear decreases in QFL%Q, QmKP%Qm and LmLvLs%Ls for the same time period. These

trends are inverted during the interval between the Late Miocene and Pliocene where there are decreases in QFL%L, LmLvLs%Lv and QmKP%P and corresponding increases in QFL%Q and QmKP%P. Note that removal of sample outliers (e.g. volcaniclastic Upper Miocene sample) from mean calculations has only a negligible effect on these trends.

DISCUSSION

Paleogeography and Depositional Environment

In general, previous workers (Field et al., 1997) have shown that the Miocene succession of the Raukumara Peninsula of North Island, New Zealand consists mainly of bathyal mudstone and deep-water sandstone punctuated by units of paralic conglomerate, and neritic sandstone and limestone. The Early Miocene depositional setting was mostly bathyal. Near the end of the Early Miocene, a large depocenter developed across the present Raukumara Peninsula (Field et al., 1997). In the beginning of the Middle Miocene, tectonism and subsidence continued, resulting in a transition from shelf sand in the west, to bathyal mudstone and sandy slope aprons in the east. At the end of the Middle Miocene, intense periods of uplift and subsidence accompanied by eustastic changes in sea level produced a combination of bathyal sandstone and mudstone along with paralic to neritic sandstone and limestone. Late Miocene to Pliocene uplift and faulting associated with motion on the Australian-Pacific plate boundary along with eustatic changes in sea level led to a variety of depositional environments along the Raukumara Peninsula (Field et al., 1997).

Paleogeographic reconstructions from Field et al. (1997, maps 17- 28) suggest that rocks within the Wairoa study area accumulated at bathyal depths (200-2000 m) or deeper from the Early Miocene to the end of the Middle Miocene. During the Late Miocene, deposition within the study area is inferred to have occurred at shelf (0–200 m) to bathyal depths. The unconformable Pliocene sequence was deposited at shelf depths. These depositional interpretations were based on analyses of facies and benthic foraminifera.

Field observations and section descriptions in this study are consistent with the interpretations of Field et al. (1997). Middle and Upper Miocene units in Sections A-C consist of mainly bioturbated calcareous mudstone with lesser thinly bedded sandstone. No well-bedded gravity-flow deposits indicative of base of slope or slope basin depositional settings were observed. The abundance of mudstone, intense bioturbation and lack of sedimentary structures in the thinly bedded sandstones indicates the probable depositional setting of these units was on the slope at bathyal depths (>200 m). Above the unconformity in Section C, the macrofossil-rich carbonate facies suggest deposition at shelf depths. The overlying sandy interval at the top of Section C is intensely bioturbated, structureless, and bioclastic rich (abundant mollusk fragments) also indicating probable deposition in a shelf setting.

Sand Provenance

Modal data from Miocene and Pliocene sandstone samples plot on the QFL ternary diagram (Fig. 12) along the boundary between the recycled orogen and dissected arc tectonic provenance fields of Dickinson et al. (1983). Mean data from subdivided units reflect a recycled orogen provenance for Lower Miocene samples whereas Middle/Upper Miocene and Pliocene samples trend into the dissected arc field. These compositions reflect the tectonic complexity of this region as the Hikurangi subduction margin evolved.

The relative tight cluster of the data on QFL and QmKP ternary diagrams (Fig. 12) suggests that similar sources contributed sand to the study area from the Miocene through to the Early Pliocene. The textural and compositional immaturity of the sandstone samples suggests a source area of high relief and close proximity to the study

area. Furthermore, the presence of fresh volcanic glass lithic fragments supports input from the magmatic arc. Paleocurrent data from Field et al. (1997) for Middle Miocene sandstone south of the study area indicate a southeast transport direction suggesting a source located to the west/northwest. The most likely sediment sources are the Torlesse basement rocks that currently crop out along the axial ranges to the west and northwest in combination with volcanic input from the magmatic arc in the Northland-Coromandel region (Fig 1). Each of these potential sources is discussed in more detail below.

According to Gosson (1986) silicic calc-alkaline arc-magmatism in North Island, New Zealand occurred throughout the Miocene and Pliocene (Fig. 1) with an average frequency of about one eruption every 25,000 years. In the Raukumara area, Gosson (1986) suggests that the majority of the volcanic ash was discharged into the sea by rivers and was likely emplaced by sediment gravity flows. These deposits represent infill of accretionary basins within a subduction complex that was likely to have been more proximal to the arc axis during the Miocene-Pliocene but was tectonically displaced (rotated) during evolution of the Hikurangi subduction zone. Thus the temporal trends in composition towards more volcanic lithic-rich sand (Fig. 12) could be explained by progressively more arc contribution through the Miocene as the arc developed. In addition to delivering arc-derived material (volcanic lithic fragments but also, to a lesser extent, feldspar and quartz phenocrysts), these rivers must have also have supplied Torlesse-derived detritus to explain the sand compositions (e.g. metamorphic lithic components).

The graywacke-dominated successions of the Torlesse composite terrane north and west of the study area are part of the Pahau subterrane, which can be further

subdivided into two late Early Cretaceous petrofacies (the Waioeka and Omaio petrofacies) as defined by Mortimer (1995) (Fig. 2). Modal data from these petrofacies are shown in Figure 13. The quartzofeldspathic graywackes of the Omaio petrofacies are slightly more quartz and feldspar-rich whereas the mafic volcaniclastic-dominated Waioeka petrofacies is lithic-rich and quartz-poor. These trends would likely persist in sand derived from these rocks, with the Omaio being the best candidate source of quartz, feldspar and metamorphic lithics.

Reservoir Potential

The study area is located within the northeast portion of Petroleum Exploration Permit 38329 that was awarded to Westech-Orion Joint Venture in May 1996. Between March 1998 and December 1999, six exploratory wells and five appraisal wells were drilled within the permit area (Davies et al., 2000). Ten wells were located approximately 30 to 50 km south of the study area and one was located roughly 20 km to the east. Drilled to depths ranging from 940 to 2320 m, each well penetrated Pliocene to Lower Miocene or Oligocene sections and was located on the crest of a seismically mapped structure. All wells found significant gas shows and two wells discovered liquid hydrocarbons in potentially commercial volumes (Davies et al., 2000). Thus the sandstone outcrops examined in this study may provide some insight into the reservoir characteristics and quality of similar units in the subsurface.

Porosity related trends are shown in Figures 14 and 15. Although the most porous samples of this study are Late Miocene and Pliocene in age, there does not appear to be a direct correlation between age and porosity as these time periods also yield some of the least porous samples. The major factors affecting overall porosity are total rock %

carbonate cement, total rock % matrix and total rock % bioclasts. Figure 15 shows that increases in any of these three components are associated with decreasing overall porosity. The calcareous nature of the Miocene mudstone could be the source for calcite cement in the sandstone with which they are interbedded. Abundant bioclasts in sandstone units provide sites for nucleation of calcite cements and promote cementation of these beds. The amount of matrix can be directly linked to bioturbative mixing. Additionally, the more quartzose (higher QFL%L) samples and those with increased volcanic lithic content tend to be more porous (Fig. 15). Squashing of sedimentary lithics was observed to decrease intergranular volume in many samples, but data on plots of sedimentary lithics versus porosity (not shown) were widely scattered and showed no distinct trend.

Descriptions of reservoir characteristics discussed above are based on porosity values and diagenetic features determined from petrographic analysis. No permeability data were collected. However, insight into the likely porosity/permeability relationships can be extrapolated from a similar study of Miocene sandstone south of the study area.

Davies et al. (2000) examined the Tunanui Sandstone, a Middle Miocene turbidite complex found in northern Hawke Bay and western Poverty Bay in outcrop and well sections. Facies within the Tunanui Sandstone range from interbedded sandstone and mudstone with thick-bedded sandstone channel fills to mud-dominated units with minor, thin-bedded, fine-grained sandstone (Davies et al., 2000). Mud-dominated facies with lesser thin-bedded, fine grained sandstone are inferred to have been deposited in a slope environment and were bypassed by the bulk of the redeposited sand whereas the thick-bedded, sand dominated facies represents deposition in a basin-floor fan (Davies, et al.,

2000). The sand dominated facies is exposed in outcrop in the southeastern coastal areas of North Island. Here the sandstone beds are 1-4 m thick but locally amalgamated up to 15 m thickness. They are fine- to very fine-grained sublitharenites with porosities up to 26% and permeabilties up to 128 mD (Davies et al., 2000). In subsurface sections, the sandstone is feldspathic litharenite (no modal data provided), medium- to thickly-bedded, moderately sorted, with subangular to subrounded grains and yield porosities of up to 18 – 22% with permeability averaging 10 mD (Davies et al., 2000). Foraminifera identified in well sections indicate a lower bathyal paleoenvironment with water depths down to 1200 m, supporting a deep basin-floor fan deposit (Davies et al., 2000).

Few of the Miocene sandstone samples in this study have greater than 10% porosity and no single bed is thick enough to have sufficient reservoir volume. However, the results of this study do provide insight into factors that could affect reservoir characteristics of equivalent Miocene units, like those studied by Davies et al. (2000). Increases of matrix in sandstone resulting from bioturbation decrease porosity. Therefore, bed thickness is an important factor in reservoir potential in these Miocene units. Thin sandstone beds of slope deposits have poor potential compared to thick sandstone beds of basin-floor fan deposits. Additionally, the occlusion of porosity in the Miocene samples may be enhanced by the presence of bioclastic debris in sandstone and the abundance of micritic carbonate in the surrounding mudstone. The porosity and permeability of thick-bedded, basin-floor deposits similar to those studied by Davies et al. (2000) could be affected by carbonate cementation. Therefore, it is important for petroleum geologists planning exploration in the Wairoa successions to conduct studies that attempt to establish the timing of petroleum migration into reservoir rock and the

timing of calcite cementation, as well as attempts to establish the pathways of fluid migration that result in carbonate cementation (e.g., regional versus local or structurally controlled pathways).

CONCLUSIONS

Results from this study are consistent with the interpretations of previous workers, summarized by Field et al. (1997), that Miocene sedimentary successions in the Raukumara Peninsula were deposited along the slope in a forearc basin setting at bathyal depths throughout the Miocene and the lower Pliocene units were most likely deposited at shelf depths after continued uplift and eustatic sea level change. Modal data in Miocene and Pliocene sandstones reflect the tectonic complexity of the region as the Hikurangi subduction margin evolved and suggest the most likely sediment sources were the Torlesse basement rocks in combination with volcanic input from the magmatic arc in the Northland-Coromandel region. Temporal trends in sandstone composition show a progressive increase in magmatic-arc contribution throughout the Miocene followed by a decrease in the abundance of volcanic debris during the early Pliocene possibly associated with a reorganization of the arc axis (Fig. 1).

The major factors affecting overall porosity in Miocene to Pliocene sandstones from this study are total rock % carbonate cement, total rock % matrix and total rock % bioclasts. A higher percentage any of these components is associated with lower overall visible porosity. Few of the sandstone samples in this study have greater than 10% porosity and no single bed is thick enough to have sufficient reservoir volume. However, the results of this study do provide insight into factors that could affect reservoir characteristics of similar Miocene units, like those studied by Davies et al. (2000). Higher matrix percentage is linked to bioturbation, with thinner beds exhibiting higher degrees of bioturbation. Therefore, bed thickness and carbonate content are important factors in reservoir potential in these Miocene units. Carbonate cementation may be

enhanced by the presence of bioclastic debris within the sandstone and the abundance of micritic carbonate within the surrounding mudstone.

REFERENCES

Adams, C., and Kelley, S., 1998, Provenance of Permian-Triassic and Ordovician metagraywacke terranes in New Zealand; evidence from Ar/Ar dating of detrital micas: Geological Society of America Bulletin, v. 110, p. 422-432.

Adams, C., Mortimer, N., Campbell, H., and Griffin, W., 2009, Age and isotopic characterization of metasedimentary rocks from the Torlesse Supergroup and Waipapa Group in central North Island, New Zealand, New Zealand Journal of Geology and Geophysics, v. 52, p. 149-170.

Ballance, P., 1976, Evolution of the upper Cenozoic magmatic arc and plate boundary in northern New Zealand: Earth and Planetary Science Letters, v. 28, p. 356 370.

Ballance, P., 1993, The New Zealand Neogene Forearc Basins, *in* Ballance, P., ed., South Pacific Sedimentary Basins, Sedimentary Basins of the World, v. 2, p. 177-193.

Berryman, K., 1993, Distribution, age and deformation of Holocene marine terraces at Mahia Peninsula, Hikurangi subduction margin, New Zealand: Tectonics, v. 12, p. 1365-1379.

Berryman, K., Ota, Y., and Hull, A., 1989, Holocene paleoseismicity in the fold and thrust belt of the Hikurangi subduction zone, eastern North Island, New Zealand: Tectonophysics, v. 163, p. 183-195.

Beu, A., 1995, Pliocene limestones and their scallops: Institute of Geological and Nuclear Sciences Monograph 10, Lower Hutt, Institute of Geological and Nuclear Sciences Ltd.

Bishop, D., Bradshaw, J., and Landis, C., 1985, Provisional terrane map of South Island, New Zealand, *in* Howell, D., eds., Tectonostratigraphic terranes of the Circum-Pacific region: Circum-Pacific Council for Energy and Mineral Resources Earth Science Series 1, p. 515-521.

Bradshaw, J., 1993, A review of the Median Tectonic Zone: terrane boundaries and terrane amalgamation near the Median Tectonic Line: New Zealand Journal of Geology and Geophysics, v. 27, p. 293-312.

Carter, L., Orpin, A., and Kuehl, S., 2010 (in press), Landscape and sediment responses from mountain source to deep ocean sink; Waipaoa Sedimentary System, New Zealand: Marine Geology.

Cole, J., 1984, Taupo-Rotorua depression – an ensialic marginal basin of North Island, New Zealand, *in* Kokelaar, B., Howells, M., eds., Marginal basin geology: volcanic and associated sedimentary and tectonic processes in modern and ancient marginal basins: Special Publication, Geological Society of London 16, p. 109-120.

Cole, J., and Lewis, K., 1981, Evolution of the Taupo-Hikurangi subduction system: Tectonophysics, v. 72, p. 1-21.

Collot, J., Delteil, J., Lewis, K., Davey, B, Lamarche, G., Audru, L., Barnes, P., Chanier, F., Chaumillion, E., Lallemand, S., de Lepinay, B., Orpin, A., Pelletier, B., Sosson, M., Toussanint, B., and Uruski, C., 1996, From oblique subduction to inter-continental transpression: Structures of the Southern Kemadec-Hikurangi Margin from multibeam bathymetry, side-scan sonar and seismic reflection: Marine Geophysical Researches, v. 18, p. 357-381.

Coombs, D., Landis, C., Norris, R., Sinton, J., Borns, D., and Craw, D., 1976, The Dun Mountain Ophiolite Belt, New Zealand, its tectonic setting, constitution, and origin with special reference to the southern portion: American Journal of Science, v. 276, p. 561-603.

Davies, E., Frederick, J., and Williams, T., 2000, East Coast drilling results: New Zealand Petroleum Conference Proceedings, March 19-22, 2000, p. 84-93.

Dickinson, W., Beard, L., Brakenridge, G., Erjavec, J., Ferguson, R., Inman, K., Knepp, R., Lindberg, F., and Ryberg, P., 1983, Provenance of North American Phanerozoic sandstones in relation to tectonic setting: Geologic Society of America Bulletin, v. 94, p. 222-235.

Dunham, R.J., 1962, Classification of carbonate rocks according to depositional textures, *in* Ham, W., ed., Classification of carbonate rocks: American Association of Petroleum Geologists Memoir 1, p. 108-121.

Field, B., and Uruski, C., and others, 1997, Cretaceous – Cenozoic Geology and Petroleum Systems of the East Coast Region, New Zealand: Institute of Geological and Nuclear Sciences Monograph 19, p. 1-301.

Folk, R., Andrew, P., and Lewis, D., 1970, Detrital sedimentary rock classification and nomenclature for use in New Zealand: New Zealand Journal of Geology and Geophysics, v. 13, p. 937-968.

Gosson, G., 1986, Miocene and Pliocene silicic tuffs in marine sediments of the East Coast Basin, New Zealand: Unpublished PhD thesis, Victoria University of Wellington.

Ingersoll, R., Fullard, T., Ford, R., Grimm, J., Pickle, J., and Sares, S., 1984, The effects of grain size on detrital modes: a test of the Gazzi-Dickinson point-counting method: Journal of Sedimentary Petrology, v. 54, p. 103-116.

Kamp, P., 1988, Tectonic geomorphology of the Hikurangi margin: surface manifestations of different modes of subduction: Zeitschrift fuer Geomorphologie, v. 69, p. 55-67.

Lamb, S., 1988, Structural studies on the East Coast of New Zealand – summary of research during 3-year UGC postdoctoral research fellowship, 1985-1987: Geological Society of New Zealand Newsletter, v. 79, p. 45-48.

Lewis, D., and Pettinga, J., 1993, The emerging, imbricate frontal wedge of the Hikurangi margin, *in* Balance, P., ed., Sedimentary Basins of the World 2, South Pacific Sedimentary Basins: Elsevier, Amsterdam.

Marsaglia, K., and Tazaki, K., 1992, Diagenetic trends in Leg 126 sandstones, In Taylor, B., Fujioka, K., et al., Proceedings of the Ocean Drilling Program, Scientific Results, 126: College Station, TX (Ocean Drilling Program), p. 125-138.

Mazengarb, C., 1982, Structure and stratigraphy at the front of the Maungahaumi Nappes, Mangatawa, Raukumara Peninsula: Unpublished MSc thesis, University of Auckland.

Mazengarb, C., 1984, The Fernside Fault: an active normal fault, Raukumara Peninsula, New Zealand: New Zealand Geological Survey Record 3, p. 98-103.

Mazengarb, C., Francis, D., and Moore, P., 1991, Sheet Y16 Tauwhareparae, Geological Map of New Zealand 1: 50000: Wellington Department of Scientific and Industrial Research.

Mazengarb, C. and Speden, I.G. (compilers), 2000, Geology of the Raukamara area: Institute of Geological and Nuclear Sciences 1:250000 Geological Map 6. 1 sheet and 60 p.

Moore, P., Hatton, Adams, A., Isaac, M., Mazengarb, C., Morgans, H., and Phillips, C., 1986, A revised Cretaceous-early Tertiary stratigraphic nomenclature for eastern North Island: New Zealand Geological Survey report G104, Wellington, Department of Scientific and Industrial Research.

Mortimer, N., 1995, Origin of the Torlesse Terrane and Coeval Rock, North Island, New Zealand: International Geology Review, v. 36, p. 891-910.

Ota, Y., Hull, A., Iso, N., Ikeda, Y., Moriya, I., and Yoshikawa, T., 1992, Holocene marine terraces on the northeast coast of North Island, New Zealand, and their tectonic significance: New Zealand Journal of Geology and Geophysics, v. 35, p. 273-288.

Paquet, F., Proust, J., Barnes, P., and Pettinga, J., 2009, Inner-forearc sequence architecture in response to climatic and tectonic forcing since 150 KA: Hawke's Bay, New Zealand: Journal of Sedimentary Research, v. 79, p. 97-124.

Pettinga, J., 1982, Upper Cenozoic structural history, coastal southern Hawke's Bay, New Zealand: New Zealand Journal of Geology and Geophysics, v. 25, p. 149-191.

Rait, G, Chanier, F., and Waters, D., 1991, Landward and seaward directed thrusting accompanying the onset of subduction beneath New Zealand: Geology, v. 19, p. 230-233

Reyners, M., and Cowan, H., 1993, The transition from subduction to continental collision: crustal structure in the north Canterbury region, New Zealand: Geophysical Journal International, v. 115, p. 1124-1136.

Rock-Color Chart Committee, 1991, Geological Society of America Rock Color Chart: distributed by the Geological Society of America, 10 p.

Thornley, S., 1996, Neogene tectonics of Raukumara Peninsula, northern Hikurangi margin, New Zealand: Unpublished PhD thesis, Victoria University of Wellington.

van der Lingen, G., 1982, Development of the North Island subduction system, New Zealand: *in* Leggett, J., ed., Trench-Forearc Geology: Blackwell Scientific Publications, Oxford, Geological Society of London Special Publication, v. 10, p. 259-272.

Walcott, R., 1978, Present tectonics and Late Cenozoic evolution of New Zealand: Geophysical Journal of the Royal Astronomical Society, v. 52, p. 137-164.

Wentworth, C., 1922, A scale of grade and class terms for clastic sediments: Journal of Geology, v. 30, p. 377-392.

Yoshikawa, T., 1988, Pattern and rate of tectonic movement and Late Quaternary geomorphic development in the Raukumara Peninsula, northeastern North Island, New Zealand: Bulletin of the Department of Geography University of Tokyo, v. 20, p. 1-28.

Yoshikawa, T., Ota, Y., Yonekura, N., Okada, A., and Iso, N., 1980, Marine terraces and their tectonic deformation on the northeast coast of the North Island, New Zealand: Geographical Review of Japan, v. 53, p. 238-262.

TABLE 1. POINT COUNT DATA AND RECALCULATED PARAMETERS

TABLE 1. POINT COUNT DATA AND RECALCULATED PARAMETERS*

Sample	Age	Qm	Qp	P	altP	K	Lsch	Lsi	Lsp	Lsa	Lma	Lmt	Lvv	G	B	Chl	M
*see Table 2 for key to symbols																	
NZ-03-HA7	MM	108	14	59	39	36	0	2	0	63	0	24	22	10	1	3	1
NZ-03-HA8	MM	107	15	90	1	31	0	4	1	97	1	12	22	7	0	0	0
NZ-03-HA10	MM	115	25	18	16	32	0	1	0	75	2	47	31	10	2	0	3
NZ-03-HA11	MM	125	12	76	0	31	28	6	0	28	0	33	39	7	4	1	0
NZ-03-HAB2	MM	120	1	44	0	52	11	5	0	50	1	50	31	3	2	0	1
NZ-03-HAB5	MM	114	0	77	2	16	1	3	0	18	2	45	35	5	2	0	1
NZ-03-HB1	UM	100	7	40	18	21	4	4	0	64	3	31	42	13	3	0	1
NZ-03-HB2	UM	97	1	86	0	33	12	2	0	16	2	33	54	4	1	0	0
NZ-03-HB4	UM	106	3	87	0	38	7	5	0	23	2	20	63	5	2	0	0
NZ-03-HB9	UM	108	3	54	0	19	5	9	0	38	0	25	76	7	1	0	0
NZ-03-HB12	UM	103	14	63	20	8	1	12	0	52	4	39	41	10	5	0	1
NZ-03-HB13	UM	127	11	114	0	15	0	4	9	49	0	11	32	10	2	1	0
NZ-03-HB17	UM	87	25	62	19	20	0	2	0	52	4	48	18	12	2	0	0
NZ-03-HB18	UM	106	15	65	12	32	1	5	0	55	3	28	26	9	2	0	2
NZ-03-HB20	UM	93	15	46	16	26	0	0	0	94	3	34	16	10	7	1	0
NZ-03-HB22	UM	102	10	50	17	24	0	6	0	43	3	12	65	12	3	1	3
NZ-03-HC1	UM	7	23	126	0	1	0	1	0	15	2	1	223	0	1	0	0
NZ-03-HC8	PI	114	21	16	2	33	0	4	0	35	2	41	14	13	7	1	0
NZ-03-HC11	PI	46	6	88	0	14	0	3	0	10	2	21	49	82	1	0	0
NZ-03-HC13	PI	81	14	48	14	20	0	3	0	44	4	46	17	2	5	5	3
NZ-03-HC14	PI	106	11	45	30	12	0	4	0	43	3	30	81	3	3	0	1
NZ-03-HC 16	PI	110	4	74	0	30	0	2	11	7	0	31	12	24	6	0	1
NZ-03-HC18	PI	93	15	86	0	24	0	9	6	53	0	20	7	14	3	0	3
NZ-03-HC21	PI	118	19	44	25	34	0	6	0	71	1	26	13	0	3	9	0
NZ-03-HC24	PI	137	13	43	46	32	0	0	0	33	0	40	19	3	5	0	3
NZ-03-HC26	PI	130	13	42	25	34	0	5	0	64	2	35	27	4	4	0	0
NZ-03-201	LM	134	13	77	1	27	0	0	8	72	0	15	29	13	1	0	0
NZ-03-202	LM	152	11	79	0	44	0	3	8	34	0	17	10	13	5	1	1
NZ-03-203	LM	127	7	93	0	24	0	1	5	50	1	26	22	20	3	2	1
NZ-03-204	LM	150	17	58	0	55	0	2	6	25	0	39	9	13	5	1	1
NZ-03-206	LM	150	17	57	0	43	0	0	2	40	0	38	12	8	4	0	0
NZ-03-212	LM	101	21	50	0	30	0	9	14	112	0	10	13	23	7	2	0
NZ-03-211	K	179	12	57	0	42	0	1	0	61	0	36	4	2	3	0	1

(continued)

TABLE 1. POINT COUNT DATA AND RECALCULATED PARAMETERS (continued)

Sample	D	Uk	Bio	O	Cm	C R	Silt	matrix	FeO2	PS1	PS2	T 1	T 2
NZ-03-HA7	0	1	17	0	97	4	9	6	2	14	6	538	400
NZ-03-HA8	0	2	10	0	138	0	53	11	1	51	9	663	400
NZ-03-HA10	0	2	20	1	134	0	16	0	2	26	1	579	400
NZ-03-HA11	0	0	6	4	158	65	0	15	0	9	0	647	400
NZ-03-HAB2	0	0	25	4	28	1	8	25	0	35	6	503	400
NZ-03-HAB5	0	15	58	6	0	0	17	281	0	18	1	717	400
NZ-03-HB1	2	2	42	3	12	0	23	49	2	55	8	549	400
NZ-03-HB2	0	0	52	7	166	1	0	7	0	5	0	579	400
NZ-03-HB4	0	0	35	4	97	0	13	80	0	2	0	592	400
NZ-03-HB9	0	0	51	4	19	0	7	49	0	24	6	505	400
NZ-03-HB12	0	3	23	1	0	0	9	0	10	91	5	515	400
NZ-03-HB13	0	2	13	0	54	0	11	7	0	8	0	480	400
NZ-03-HB17	0	2	47	0	3	0	121	325	7	42	18	916	400
NZ-03-HB18	0	2	36	1	93	0	56	89	0	4	1	643	400
NZ-03-HB20	0	2	37	0	18	0	25	32	0	102	19	596	400
NZ-03-HB22	0	3	46	0	5	0	49	208	19	59	11	751	400
NZ-03-HC1	0	0	1	0	0	0	7	124	0	89	87	708	401
NZ-03-HC8	0	1	95	1	74	1	9	63	0	10	3	560	400
NZ-03-HC11	0	1	66	11	5	0	7	132	0	26	13	583	400
NZ-03-HC13	0	1	90	3	34	0	61	238	0	6	14	753	400
NZ-03-HC14	0	3	19	6	0	0	7	15	0	103	33	558	400
NZ-03-HC 16	0	3	83	2	0	0	58	271	0	8	6	743	400
NZ-03-HC18	0	2	65	0	73	0	2	1	2	4	0	482	400
NZ-03-HC21	0	2	25	4	108	1	4	0	0	1	1	515	400
NZ-03-HC24	0	0	25	1	0	3	25	143	13	55	4	643	400
NZ-03-HC26	0	1	11	3	100	6	4	0	10	2	1	523	400
NZ-03-201	0	0	10	0	74	0	39	8	0	55	3	579	400
NZ-03-202	1	2	19	0	0	6	77	155	2	70	3	713	400
NZ-03-203	2	1	15	0	61	0	26	32	1	1	0	521	400
NZ-03-204	0	1	18	0	34	0	30	48	1	9	0	522	400
NZ-03-206	0	0	29	0	14	0	37	74	2	23	3	553	400
NZ-03-212	0	2	6	0	10	0	4	39	1	21	3	478	400
NZ-03-211	0	2	0	0	0	0	76	360	0	0	1	837	400

(continued)

TABLE 1. POINT COUNT DATA AND RECALCULATED PARAMETERS (continued)

Sample	QFL%Q	QFL%F	QFL%L	QmKP%Qm	QmKP%K	QmKP%P	LmLvLs%Lm	LmLvLs%Lv	LmLvLs%Ls	% Porosity
NZ-03-HA7	33.2	36.5	30.2	44.6	14.9	40.5	21.6	19.8	58.6	3.7
NZ-03-HA8	32.0	32.0	36.0	46.7	13.5	39.7	9.5	16.1	74.5	9.0
NZ-03-HA10	38.7	18.2	43.1	63.5	17.7	18.8	31.4	19.9	48.7	4.7
NZ-03-HA11	36.2	28.3	35.4	53.9	13.4	32.8	24.6	29.1	46.3	1.4
NZ-03-HAB2	33.2	26.3	40.5	55.6	24.1	20.4	34.5	20.9	44.6	8.2
NZ-03-HAB5	36.4	30.4	33.2	54.5	7.7	37.8	45.2	33.7	21.2	2.6
NZ-03-HB1	32.0	23.7	44.3	55.9	11.7	32.4	23.0	28.4	48.6	11.5
NZ-03-HB2	29.2	35.4	35.4	44.9	15.3	39.8	29.4	45.4	25.2	0.9
NZ-03-HB4	30.8	35.3	33.9	45.9	16.5	37.7	18.3	52.5	29.2	0.3
NZ-03-HB9	32.9	21.7	45.4	59.7	10.5	29.8	16.3	49.7	34.0	5.9
NZ-03-HB12	32.8	25.5	41.7	53.1	4.1	42.8	28.9	27.5	43.6	18.6
NZ-03-HB13	37.1	34.7	28.2	49.6	5.9	44.5	10.5	30.5	59.0	1.7
NZ-03-HB17	33.2	30.0	36.8	46.3	10.6	43.1	41.9	14.5	43.5	6.6
NZ-03-HB18	34.8	31.3	33.9	49.3	14.9	35.8	26.3	22.0	51.7	0.8
NZ-03-HB20	31.5	25.7	42.9	51.4	14.4	34.3	25.2	10.9	63.9	20.3
NZ-03-HB22	33.7	27.4	38.9	52.8	12.4	34.7	11.6	50.4	38.0	9.3
NZ-03-HC1	7.5	31.8	60.7	5.2	0.7	94.0	1.2	92.1	6.6	24.9
NZ-03-HC8	47.9	18.1	34.0	69.1	20.0	10.9	44.8	14.6	40.6	2.3
NZ-03-HC11	21.8	42.7	35.6	31.1	9.5	59.5	27.1	57.6	15.3	6.7
NZ-03-HC13	32.6	28.2	39.2	49.7	12.3	38.0	43.9	14.9	41.2	2.7
NZ-03-HC14	32.1	23.8	44.1	54.9	6.2	38.9	20.5	50.3	29.2	24.4
NZ-03-HC 16	40.6	37.0	22.4	51.4	14.0	34.6	49.2	19.0	31.7	1.9
NZ-03-HC18	34.5	35.1	30.4	45.8	11.8	42.4	21.1	7.4	71.6	0.8
NZ-03-HC21	38.4	28.9	32.8	53.4	15.4	31.2	23.1	11.1	65.8	0.4
NZ-03-HC24	41.3	33.3	25.3	53.1	12.4	34.5	43.5	20.7	35.9	9.2
NZ-03-HC26	37.9	26.8	35.3	56.3	14.7	29.0	27.8	20.3	51.9	0.6
NZ-03-201	39.1	27.9	33.0	56.1	11.3	32.6	12.1	23.4	64.5	10.0
NZ-03-202	45.5	34.4	20.1	55.3	16.0	28.7	23.6	13.9	62.5	10.2
NZ-03-203	37.6	32.9	29.5	52.0	9.8	38.1	25.7	21.0	53.3	0.2
NZ-03-204	46.3	31.3	22.4	57.0	20.9	22.1	48.1	11.1	40.7	1.7
NZ-03-206	46.5	27.9	25.6	60.0	17.2	22.8	41.3	13.0	45.7	4.7
NZ-03-212	33.9	22.2	43.9	55.8	16.6	27.6	6.3	8.2	85.4	5.0
NZ-03-211	48.7	25.3	26.0	64.4	15.1	20.5	35.3	3.9	60.8	0.1

TA BLE 2. POINT-COUNT CATEGORIES AND DEFINITIONS OF RECALCULATED PARAMETERS

Counted categories

Qm	Monocrystalline quartz
Qp	Polycrystalline quartz
P	Plagioclase
altP	Altered plagioclase
K	Potassium feldspar
Lsch	Sedimentary chert lithic
Lsi	Siltstone lithic
Lsp	Carbonate lithic
Lsa	Shale lithic
Lma	Quartz-mica-feldspar lithic
Lmt	Quartz-mica tectonite lithic
Lvv	Volcanic lithic
G	Glauconite pellet
B	Biotite
Chl	Chlorite
M	Muscovite
D	Dense mineral
Uk	Unknown grain
Bio	Bioclast
Cm	Carbonate cement
O	Other
CR	Clay rim cement
Silt	Silt sized grain
Fe02	Iron oxide cement
PS	Pore space (PS1 = intergranular; PS2 = intragranular)
Matrix	Clay matrix

Recalculated Parameters

QFL%Q = 100* Q/(Q+F+L)
QFL%F = 100* F/(Q+F+L)
QFL%L = 100* L/(Q+F+L)
QmKP%Qm = 100* Qm/ (Qm+K+P)
QmKP%K = 100* K/ (Qm+K+P)
QmKP%P = 100* P/ (Qm+K+P)
LmLvLs%Lm = 100* Lm/ (Lm+Lv+Ls)
LmLvLs%Lv = 100* Lv/ (Lm+Lv+Ls)
LmLvLs%Ls = 100* Ls/ (Lm+Lv+Ls)
Porosity = 100* (PS1+PS2)/T1

Note: Q = (Qm+QP); L = (Lsch+Lsi+Lsp+Lsa+Lma+Lmt+Lvv); F = (P+altP+K);
Lm = (Lma+Lmt); Ls = (Lsch+Lsi+Lsp+Lsa)
T1 = Total points counted (sand-sized grains + interstitial components)
T2 = Total sand sized grains counted
K = Cretaceous, LM = Lower Miocene, MM = Middle Miocene, UM = Upper Miocene, Pl = Pliocene

APPENDIX B: FIGURE CAPTIONS

Figure 1. Location map and cross section showing study area and various geomorphic, volcanic and tectonic features in North Island, New Zealand (simplified from Paquet, et al., (2007)). Miocene arc-related features shown in black triangles; Pliocene are-related features shown in white triangles (modified from Ballance (1993)).

Figure 2. Geologic map of a portion of the Raukumara Region, North Island, New Zealand (structure and stratigraphy simplified from Mazengarb and Speeden (2000)). Map shows locations of Middle/Upper Miocene measured Sections A, B and C, Cretaceous to Lower Miocene outcrop sample sites (from east to west: NZ03-211, -208, -210, -207, -212, -206, -203 and -204, -201 and -202) and in upper left corner, the inferred distribution of the Omaio and Waieoka petrofacies of the Pahau subterrane from the Torlesse Supergroup (Adams et al., 2009).

Figure 3. Inset from Figure 2 showing detailed locations of roadcut exposures along Highway 36 (a.k.a. Tiniroto Road) used in this study for measured Sections A, B and C.

Figure 4. Graphic sections showing correlation of previous work from Gosson, (1986, left) to measured Sections A, B and C (right) from this study. Section A and B correlations are based on map projections; Section C correlation is based on lithology (e.g., Pliocene packstone). Figure also shows epoch, New Zealand Stages (Tk = Kapitean), lithologic group and fossil data. Fossils include (Gosson, 1986): Bcc, Bolivinita Compressa; Bp, Bolivinita pohana; Bq, Bolivinita quadrilateral; Bz, Bolivinita pliozea; Gd, Globoquadrina dehiscens; Gm, Globortalia menardi; Gmc, Globorotalia miozea conoidea; Gmm, Globorotalia mayeri mayeri; Lt, Loxostomum truncatum; Ss, Sigmoilopsis schlumbergeri.

Figure 5. Schematic stratigraphic sections (weathered profiles) showing thickness, lithology and sample locations of measured Sections A (5A), B (5B), and C (5C).

Figure 6. Field photos of measured Sections A, B and C. A. and B. Roadside exposure of a portion of Section A. C. Roadside exposure of a portion of Section B. D. Alternating mudstone and sandstone beds in Section B. (Jacob staff for scale). E. Roadside exposure of a portion of Section C showing Upper Miocene units (gray) and unconformably overlying Pliocene units (yellow and brown) with Jacob staff for scale.

Figure 7. Photomicrographs of representative sandstone samples from Section A showing thin-sections in plane light (left) and with nicols crossed (right). Samples are impregnated with blue epoxy to identify pore space and

stained for feldspar identification: pink = plagioclase; yellow = potassium feldspar. A. and B. Sample HA11: 1.4% porosity; C. and D. Sample HA7: 3.7% porosity; E and F. Sample HA10: 4.7% porosity. Note the high percentage of carbonate cement.

Figure 8. Photomicrographs of representative mudstone samples from Sections A, B and C showing thin-sections in plane light (left) and with nicols crossed (right). Samples are impregnated with blue epoxy to identify pore space. A. and B. Sample HA2; C. and D. Sample HB 8; E. and F. Sample HC 3. Note variable carbonate content of matrix as indicated by birefringence and trace amounts of visible porosity.

Figure 9. Photomicrographs of representative sandstone samples from Section B showing thin-sections in plane light (left) and with nicols crossed (right). Samples are impregnated with blue epoxy to identify pore space and stained for feldspar identification: pink = plagioclase; yellow = potassium feldspar. A. and B. Sample HB2: 0.9% porosity; C. and D. sample HB1: 11.5% porosity; E and F. sample HB20: 20.3% porosity. Note the lower porosity in the matrix-rich sample HB2.

Figure 10. Photomicrographs of representative sandstone samples from Section C showing thin-sections in plane light (left) and with nicols crossed (right). Samples are impregnated with blue epoxy to identify pore space and stained for feldspar identification: pink = plagioclase; yellow = potassium feldspar. A. and B. Sample HC21: 0.4% porosity; C. and D. sample HC24: 9.2% porosity; E and F. sample HC1: 24.9% porosity. Note the high porosity in the more volcaniclastic sample HC1 with common plagioclase crystals and vesicular glass.

Figure 11. Photomicrographs of fossiliferous packstone from Section C showing thin-sections in plane light (left) and with nicols crossed (right). Samples are impregnated with blue epoxy to identify pore space. A. and B. Sample HA9; C. and D. Sample HA10. Note green glauconite pellets and large bioclasts.

Figure 12. QFL, QmKP and LmLvLs ternary plots of recalculated parameters for point count data (left) and mean values for data sets (right) from selected sandstone samples. Each point (left) represents data from 400 sand-sized grains counted using the Gazzi-Dickinson method. QFL plot also shows provenance fields after (Dickinson et al., 1983). Temporal trends in mean values (symbols keyed to age) shown with arrows. A. QFL: quartz-feldspar-lithics; B. LmLvLs: metamorphic lithics-volcanic lithics-sedimentary lithics; C. QmKP: monocrystalline quartz-potassium feldspar-plagioclase feldspar.

Figure 13. QFL ternary plots for study area sandstone samples and potential Torlesse metasedimentary source rocks. A. Mean values from sandstones in this study. Polygons represent one standard deviation about the mean. B. Omaio (black) and Waieoka (red) petrofacies sandstones from the Pahau subterrane. Small ellipses represent 95% confidence regions of each age population mean and large ellipses represent 95% confidence regions of all data in each age population (modified from Adams et al. (2009)). pf = petrofacies.

Figure 14. Histogram showing variation in percent porosity of sandstone samples by age.

Figure 15. Scatter plots showing trends of various components vs. porosity based on sandstones point-counted in this study.

APPENDIX C: FIGURES

FIGURE 1

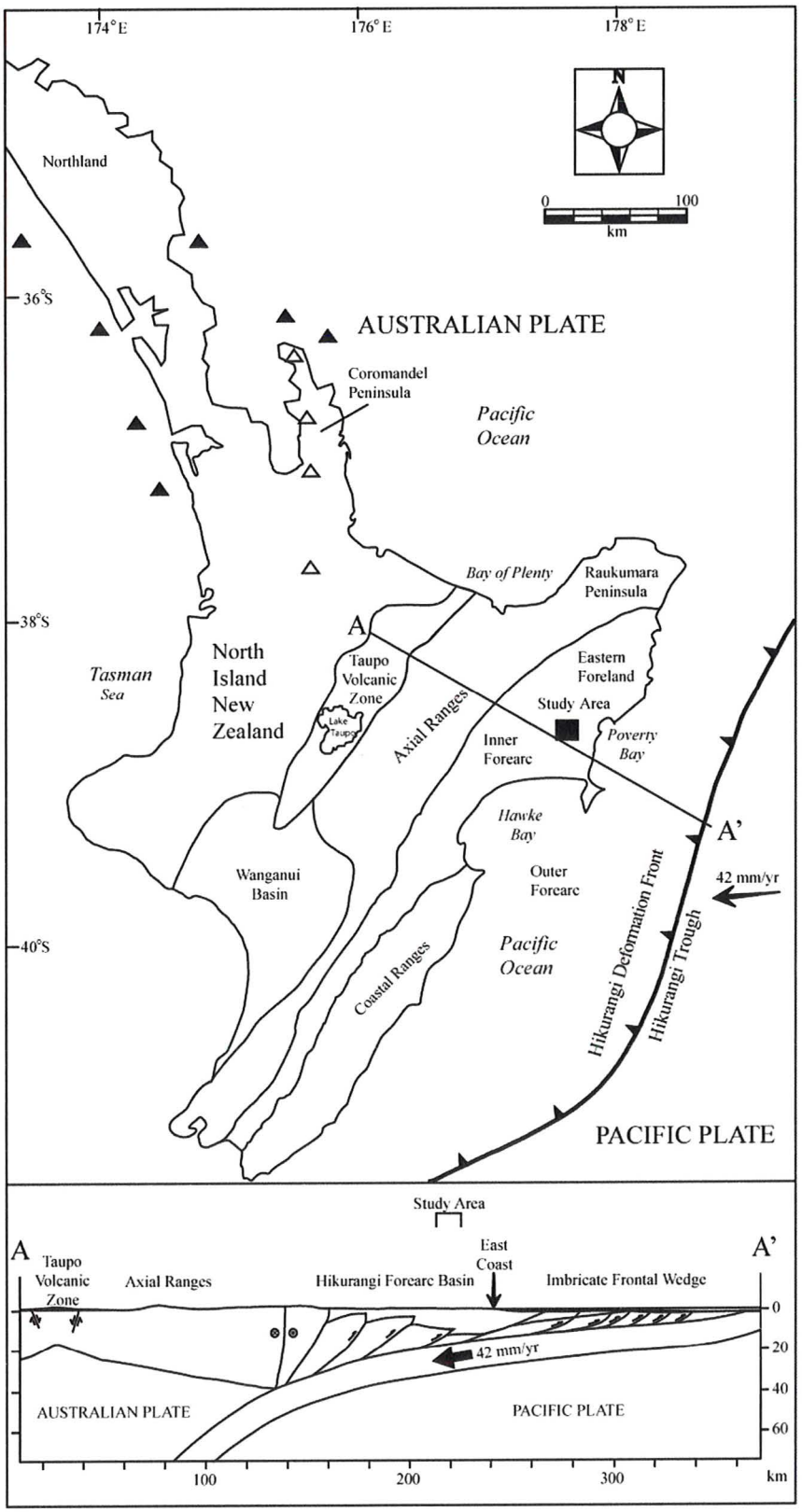

FIGURE 2

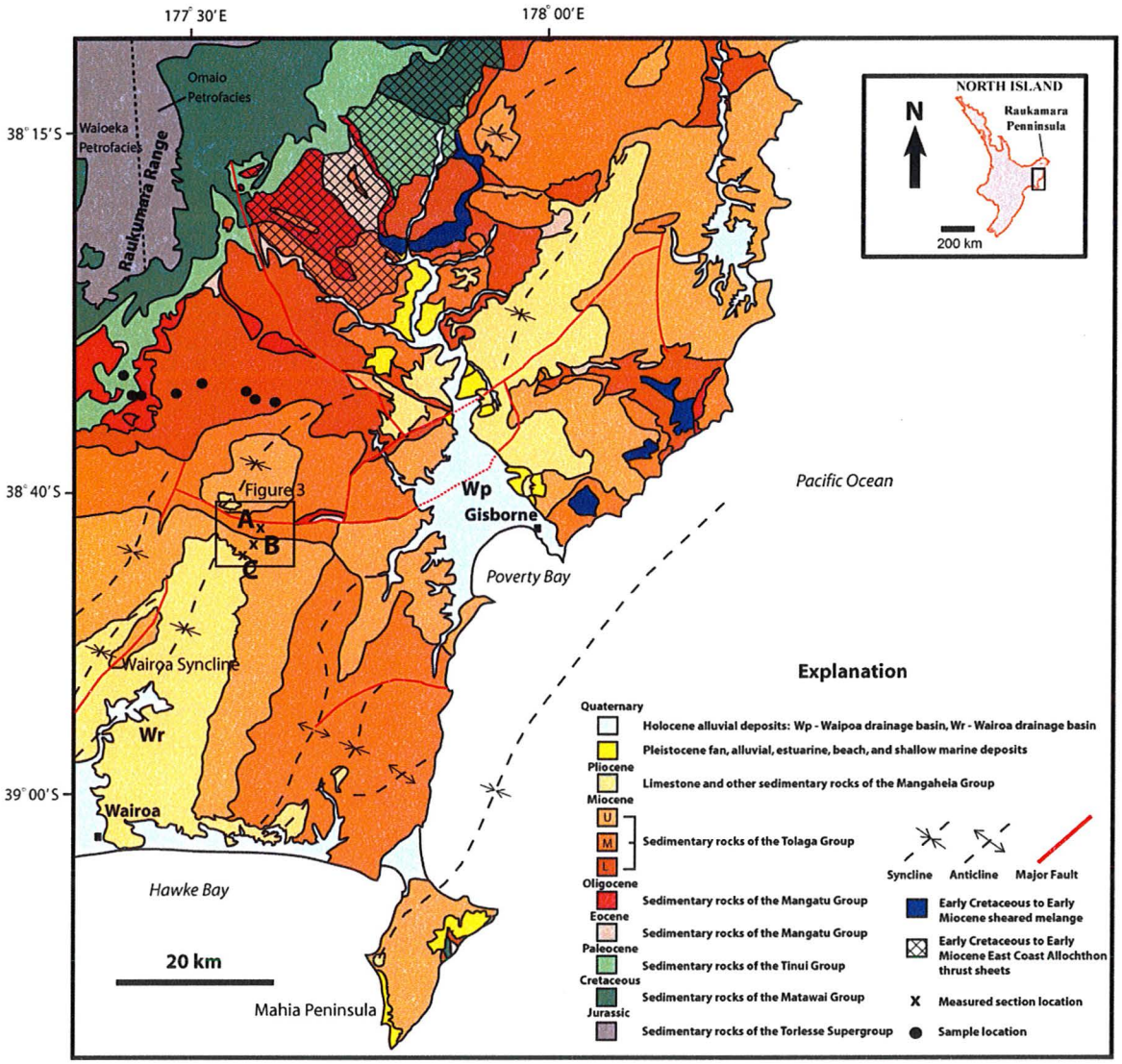
177° 30'E
178° 00'E
38° 15'S
38° 40'S
39° 00'S
Omaio Petrofacies
Waioeka Petrofacies
Raukumara Range
NORTH ISLAND
N
Raukamara Peninsula
200 km
Figure 3
A
B
C
Wp
Gisborne
Poverty Bay
Pacific Ocean
Wairoa Syncline
Wr
Wairoa
Hawke Bay
20 km
Mahia Peninsula
Explanation
Quaternary
Holocene alluvial deposits: Wp - Waipoa drainage basin, Wr - Wairoa drainage basin
Pleistocene fan, alluvial, estuarine, beach, and shallow marine deposits
Pliocene
Limestone and other sedimentary rocks of the Mangaheia Group
Miocene
U
M
L
Sedimentary rocks of the Tolaga Group
Oligocene
Sedimentary rocks of the Mangatu Group
Eocene
Sedimentary rocks of the Mangatu Group
Paleocene
Sedimentary rocks of the Tinui Group
Cretaceous
Sedimentary rocks of the Matawai Group
Jurassic
Sedimentary rocks of the Torlesse Supergroup
Syncline
Anticline
Major Fault
Early Cretaceous to Early Miocene sheared melange
Early Cretaceous to Early Miocene East Coast Allochthon thrust sheets
Measured section location
Sample location

FIGURE 3

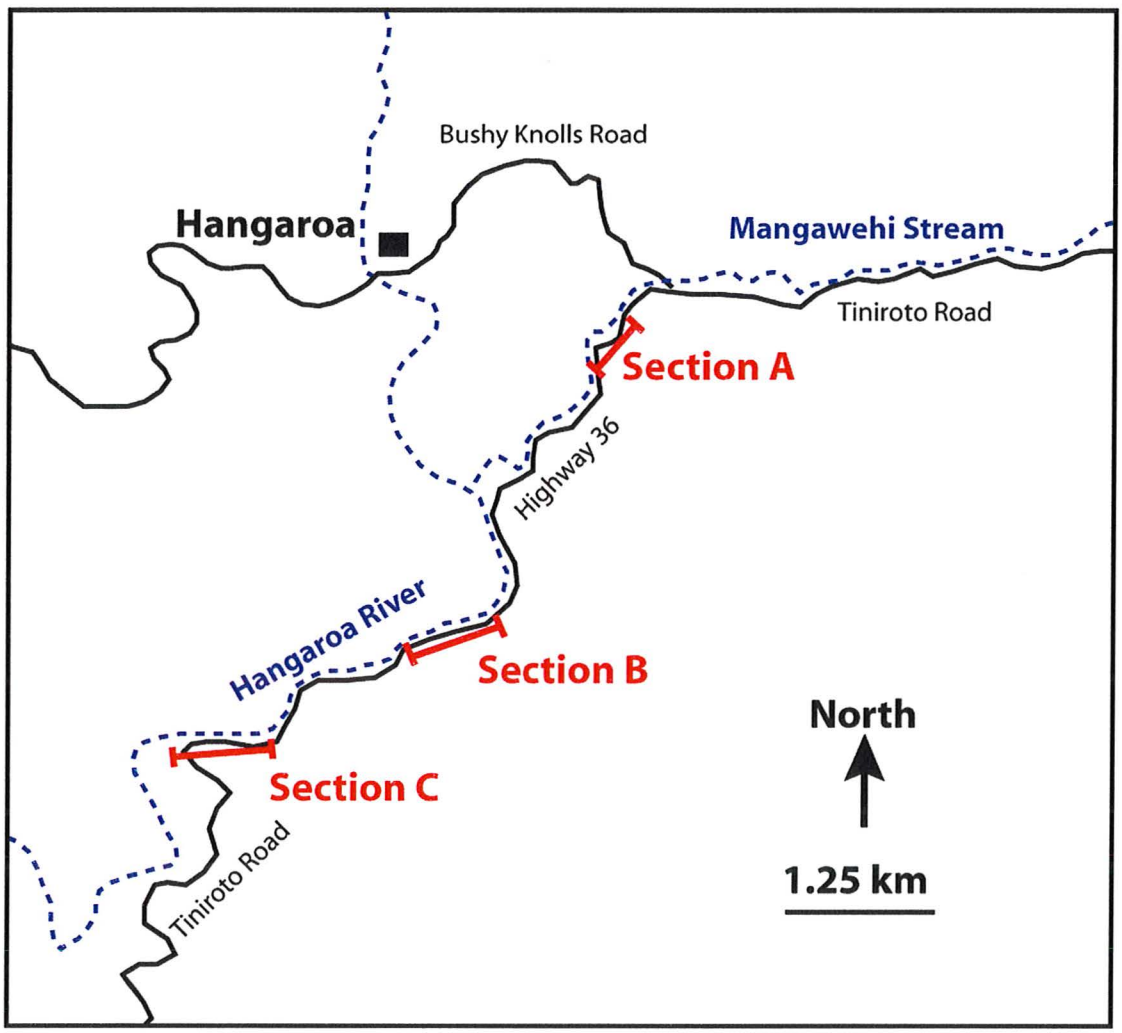
Bushy Knolls Road
Hangaroa
Mangawehi Stream
Tiniroto Road
Section A
Highway 36
Hangaroa River
Section B
Section C
Tiniroto Road
North
1.25 km

FIGURE 4

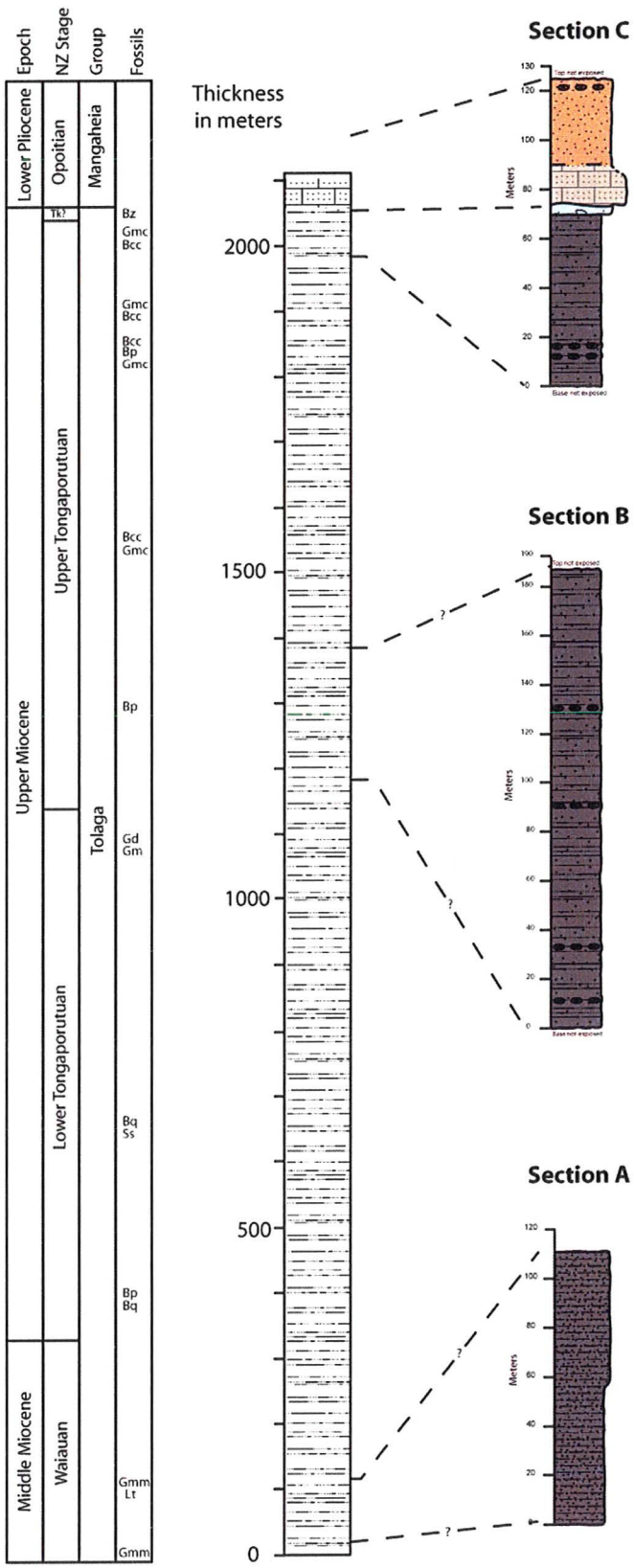
Epoch
NZ Stage
Group
Fossils
Lower Pliocene
Upper Miocene
Middle Miocene
Opoitian
Upper Tongaporutuan
Lower Tongaporutuan
Waiauan
Mangaheia
Tolaga
Tk?
Bz
Gmc
Bcc
Gmc
Bcc
Bcc
Bp
Gmc
Bcc
Gmc
Bp
Gd
Gm
Bq
Ss
Bp
Bq
Gmm
Lt
Gmm
Thickness
in meters
2000
1500
1000
500
0
Section C
Section B
Section A
Meters
Top not exposed
Base not exposed
?

FIGURE 5A

Section A

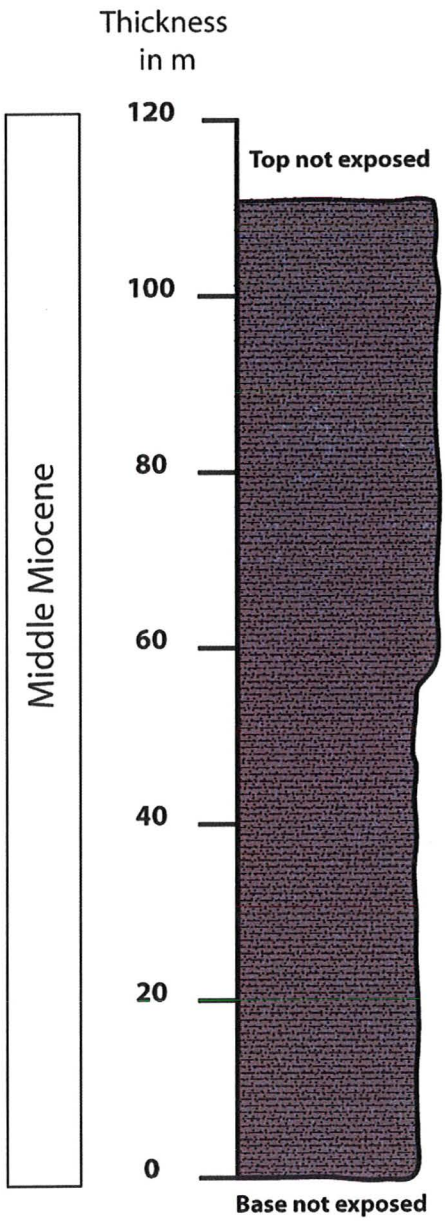

Sample Location	Description
HA9	Entire section consists of light olive gray, bioturbated mudstone with rare macrofossils interbedded with fine- to medium-grained, centimeter- to decimeter-bedded sandstone
HA8*	
HA10*	
HA11*	
HA7*	
HA6	
HA5	
HA4	
HA3	
HA2	
HA1	* = point counted sample

FIGURE 5B

Section B

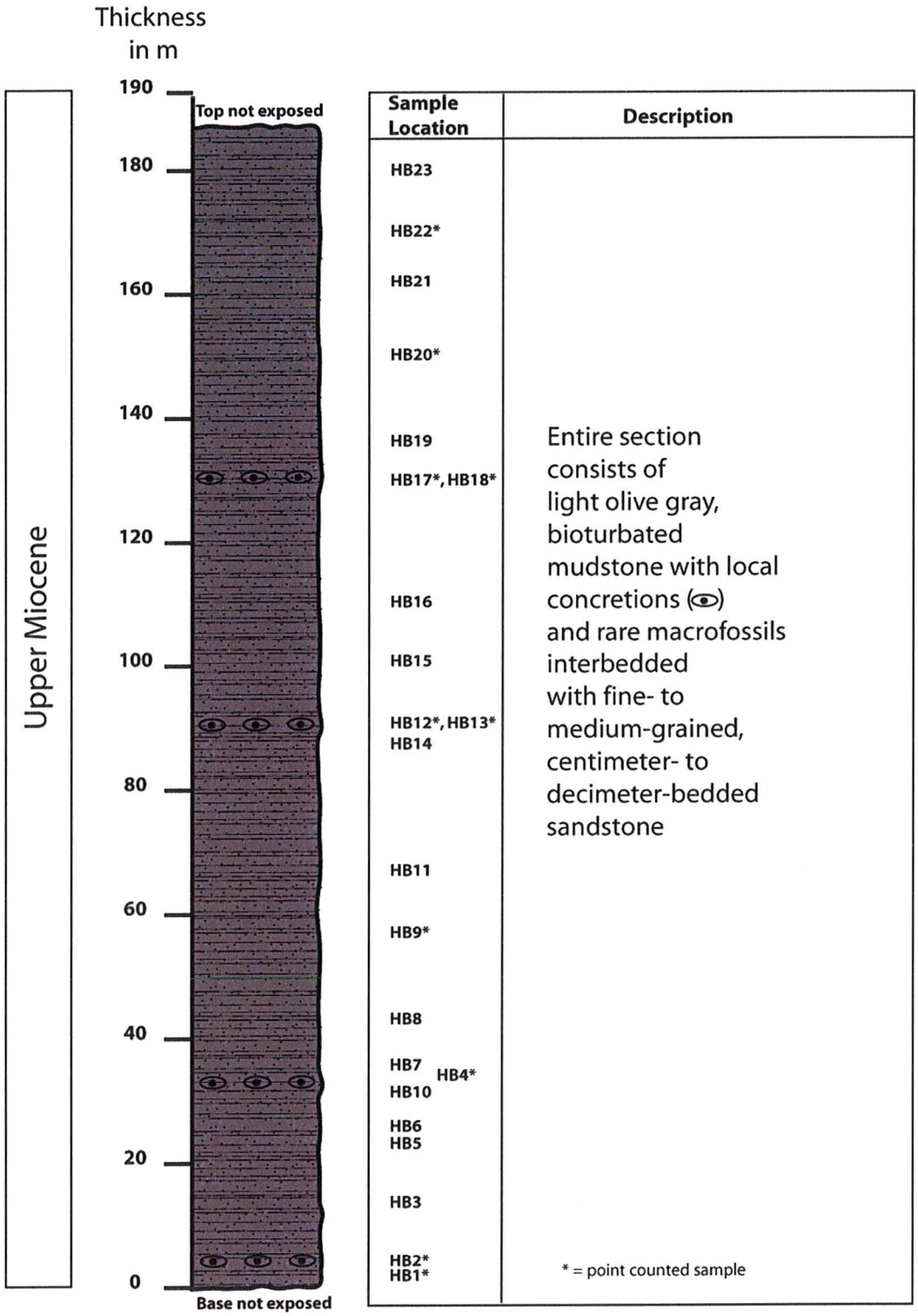

FIGURE 5C

Section C

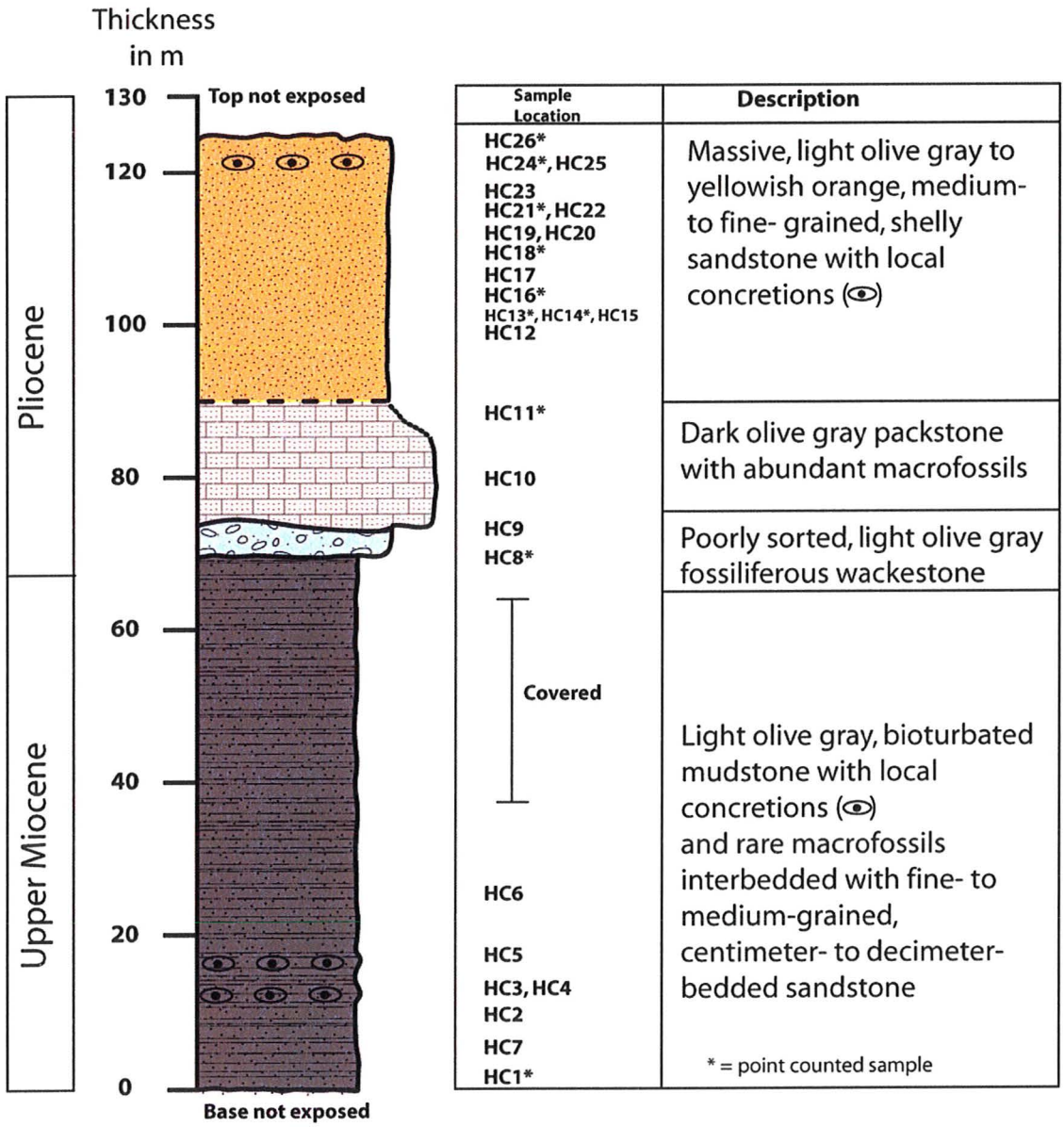

FIGURE 6

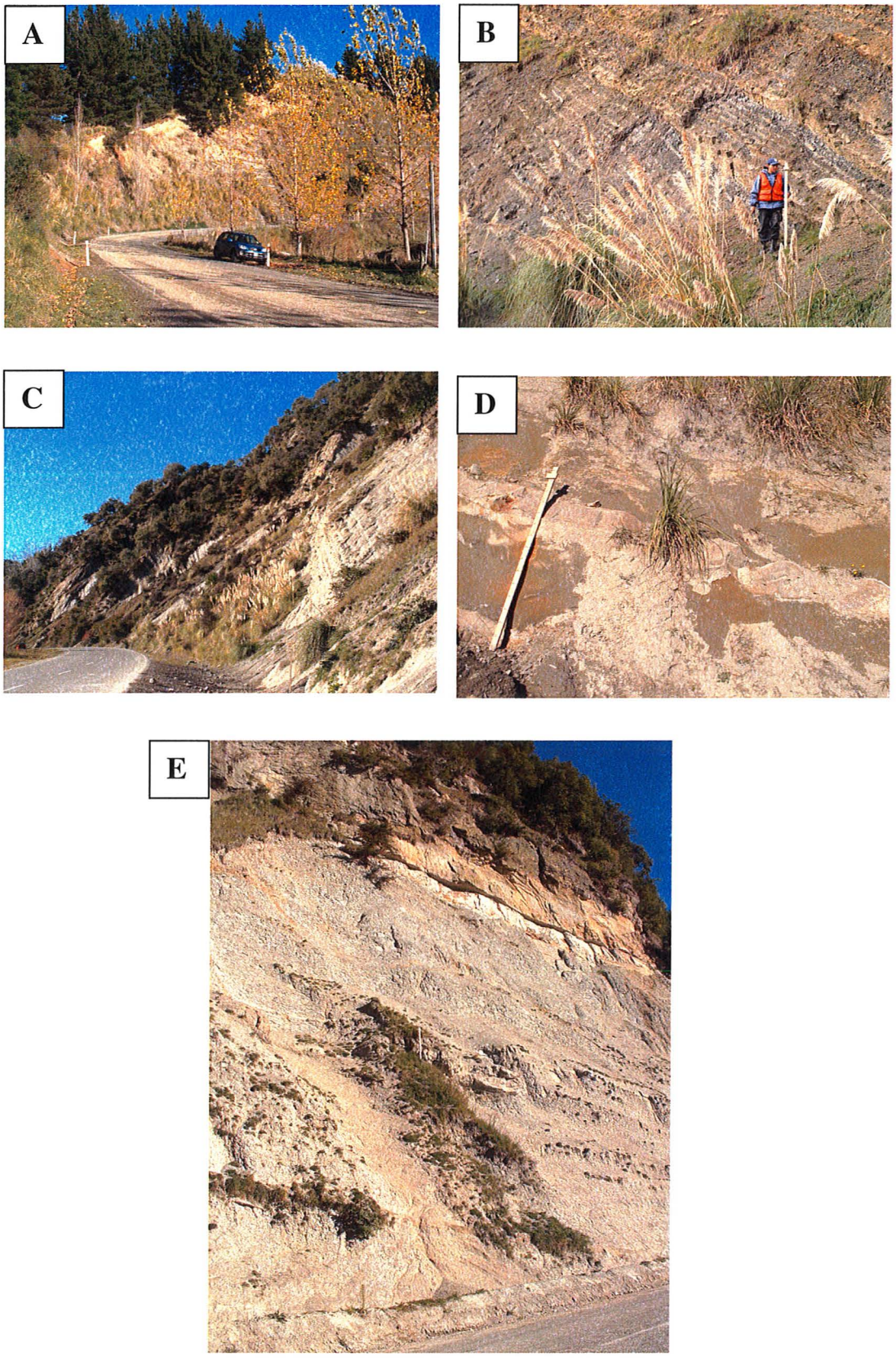

FIGURE 7

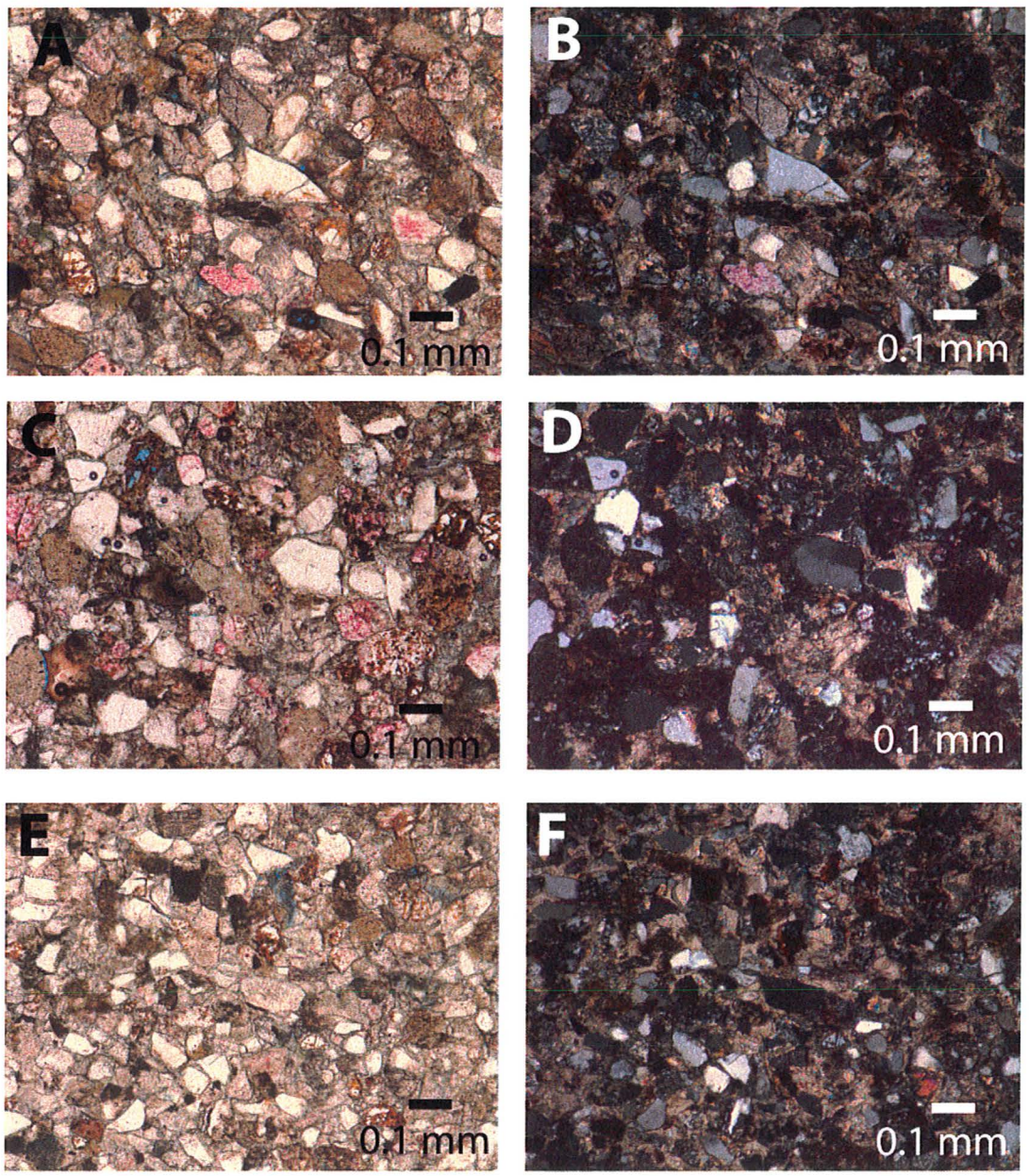

FIGURE 8

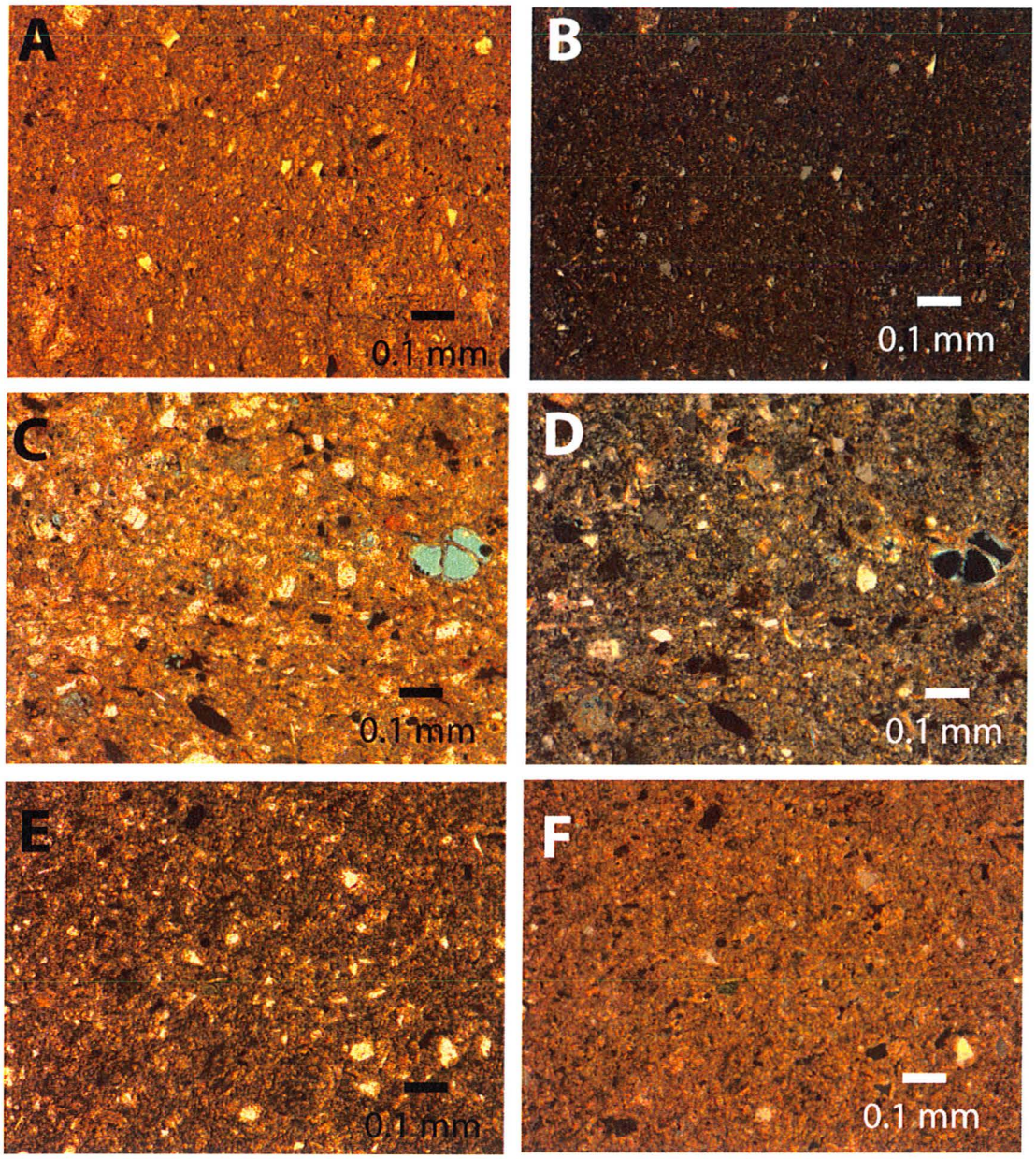

FIGURE 9

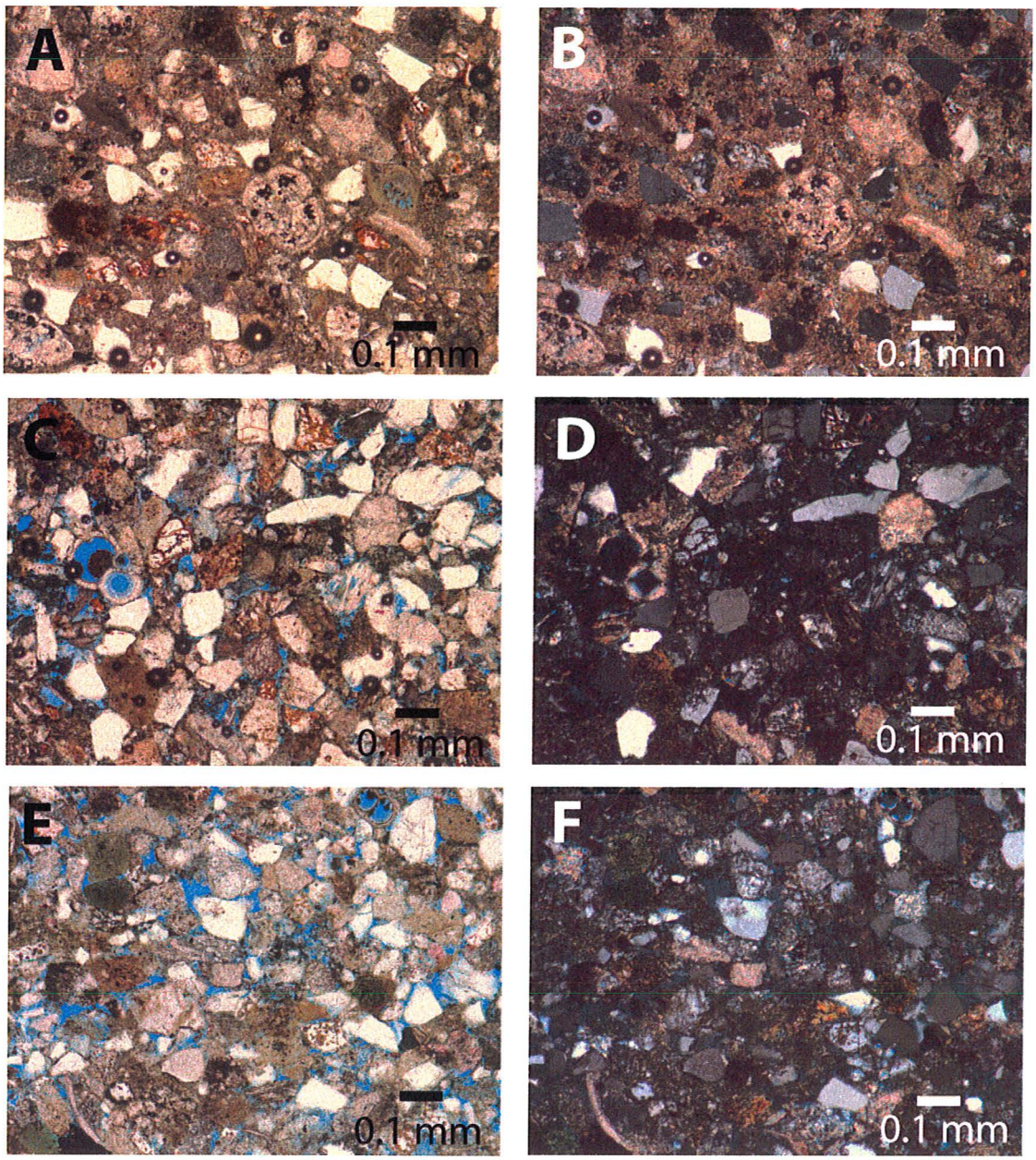

FIGURE 10

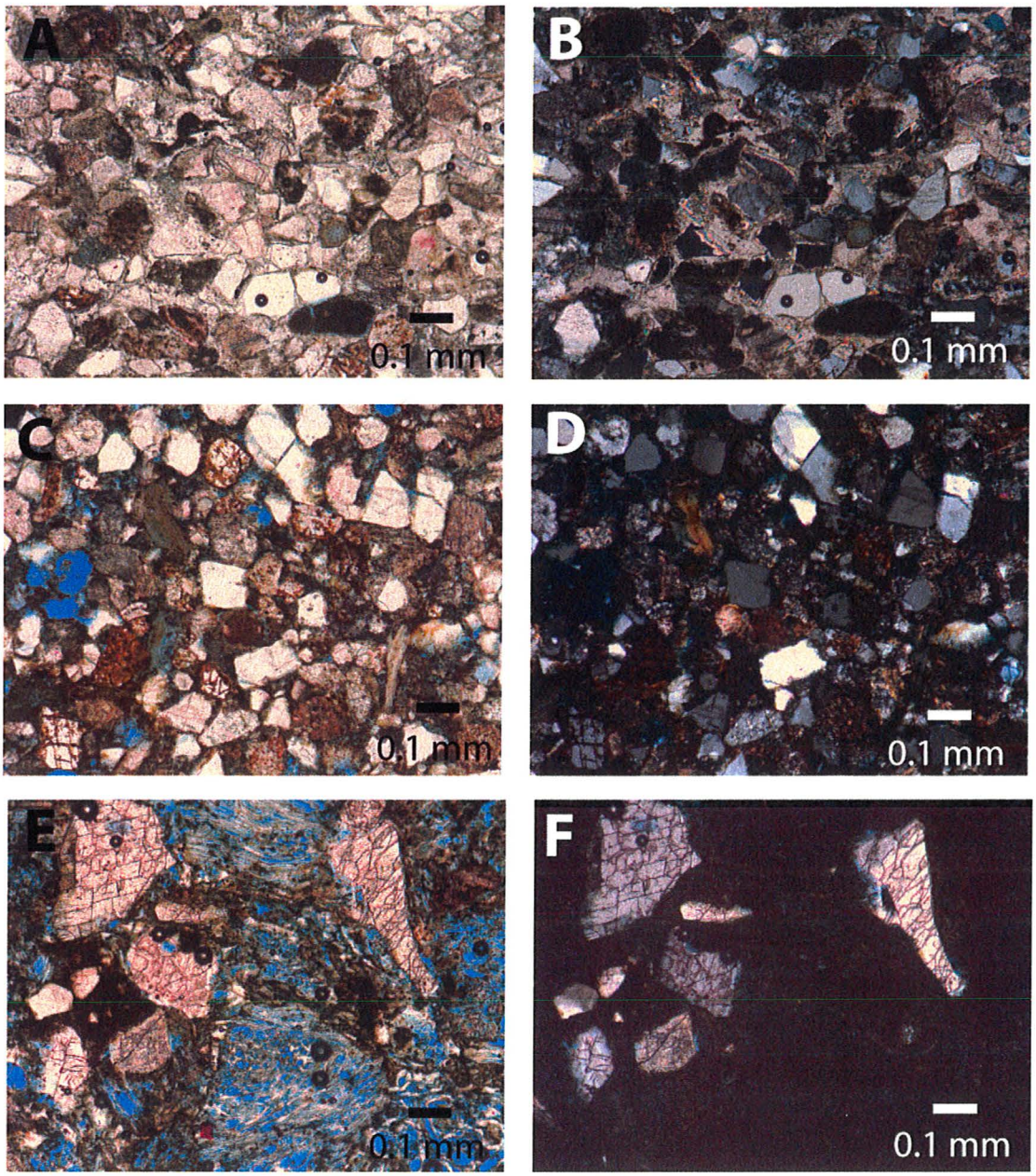

FIGURE 11

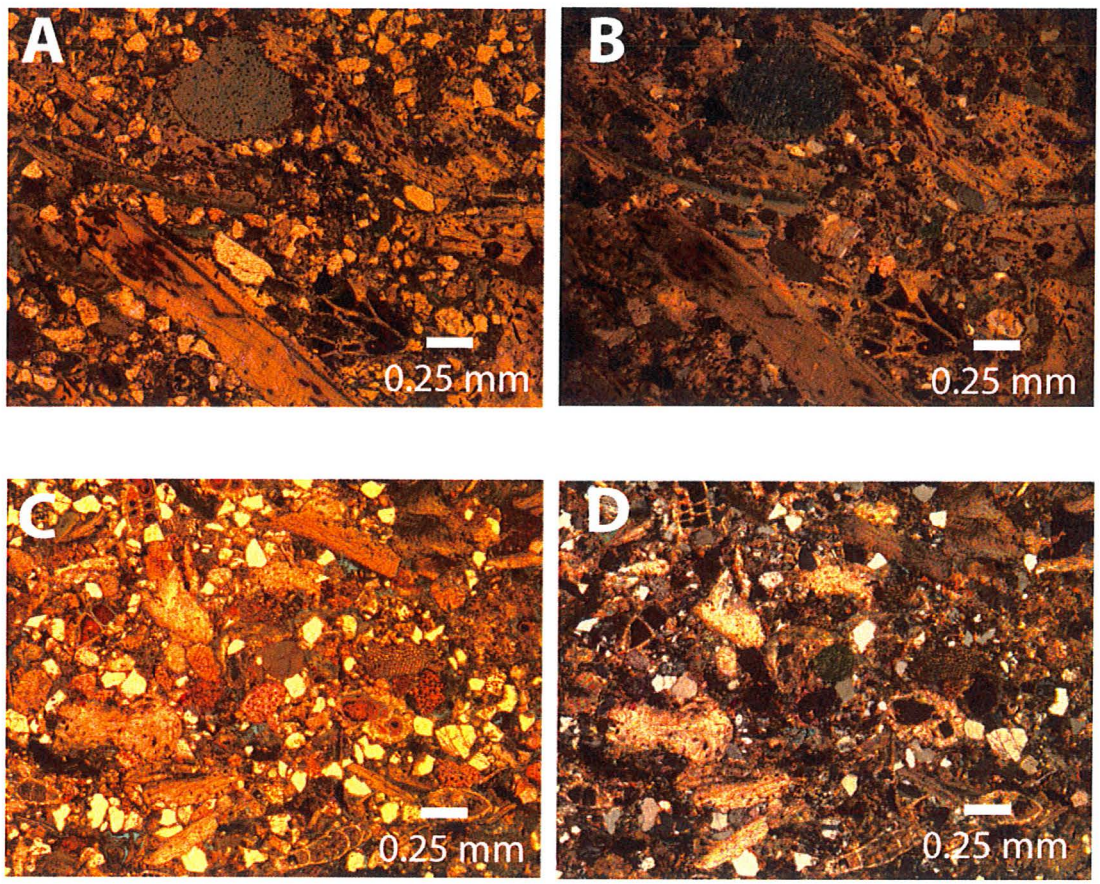

FIGURE 12

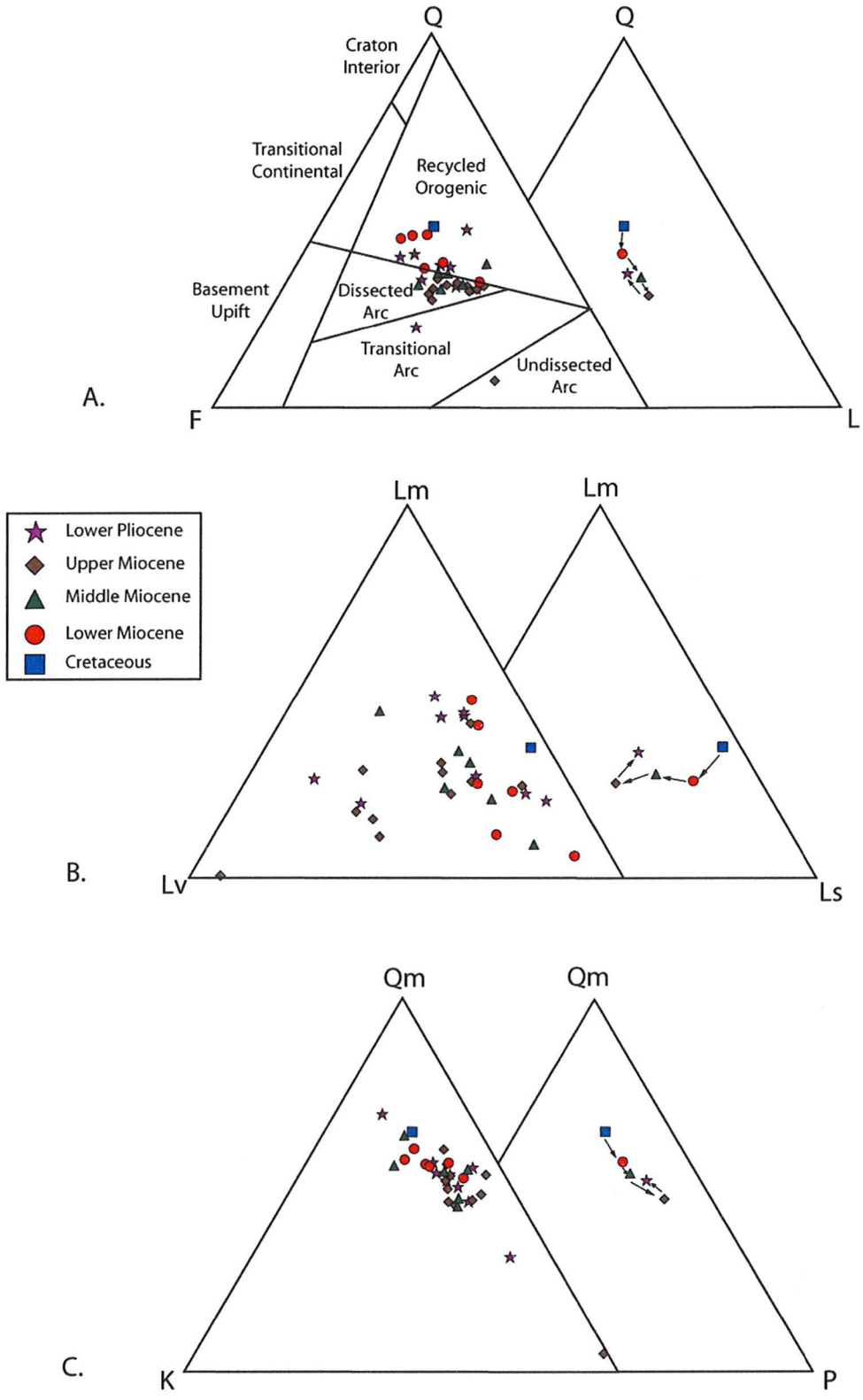
A.
Q
Q
Craton
Interior
Transitional
Continental
Recycled
Orogenic
Basement
Upift
Dissected
Arc
Transitional
Arc
Undissected
Arc
F
L
B.
Lm
Lm
Lower Pliocene
Upper Miocene
Middle Miocene
Lower Miocene
Cretaceous
Lv
Ls
C.
Qm
Qm
K
P

FIGURE 13

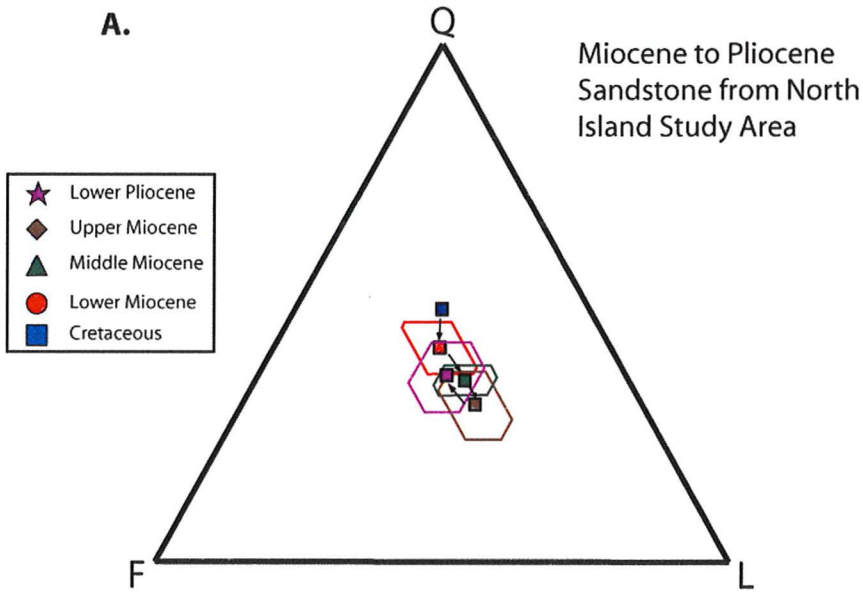
A.
Q
Miocene to Pliocene Sandstone from North Island Study Area
Lower Pliocene
Upper Miocene
Middle Miocene
Lower Miocene
Cretaceous
F
L

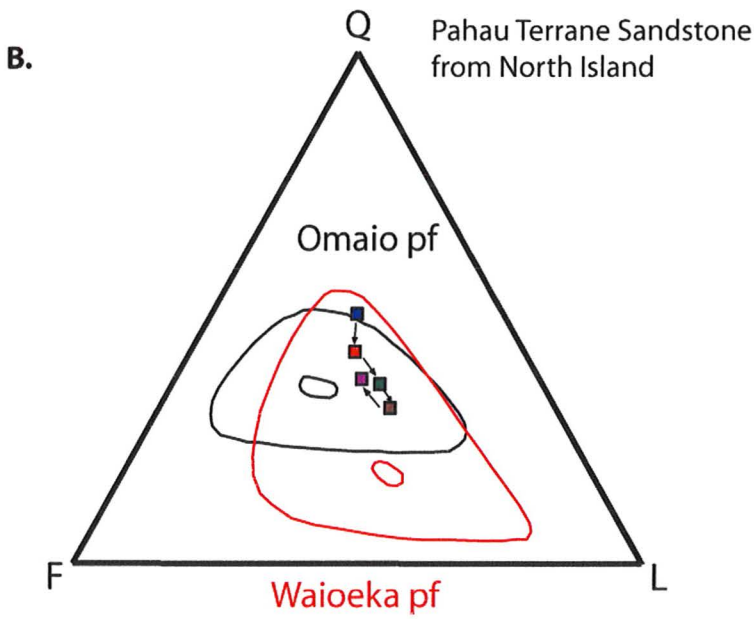
B.
Q
Pahau Terrane Sandstone from North Island
Omaio pf
F
L
Waioeka pf

FIGURE 14

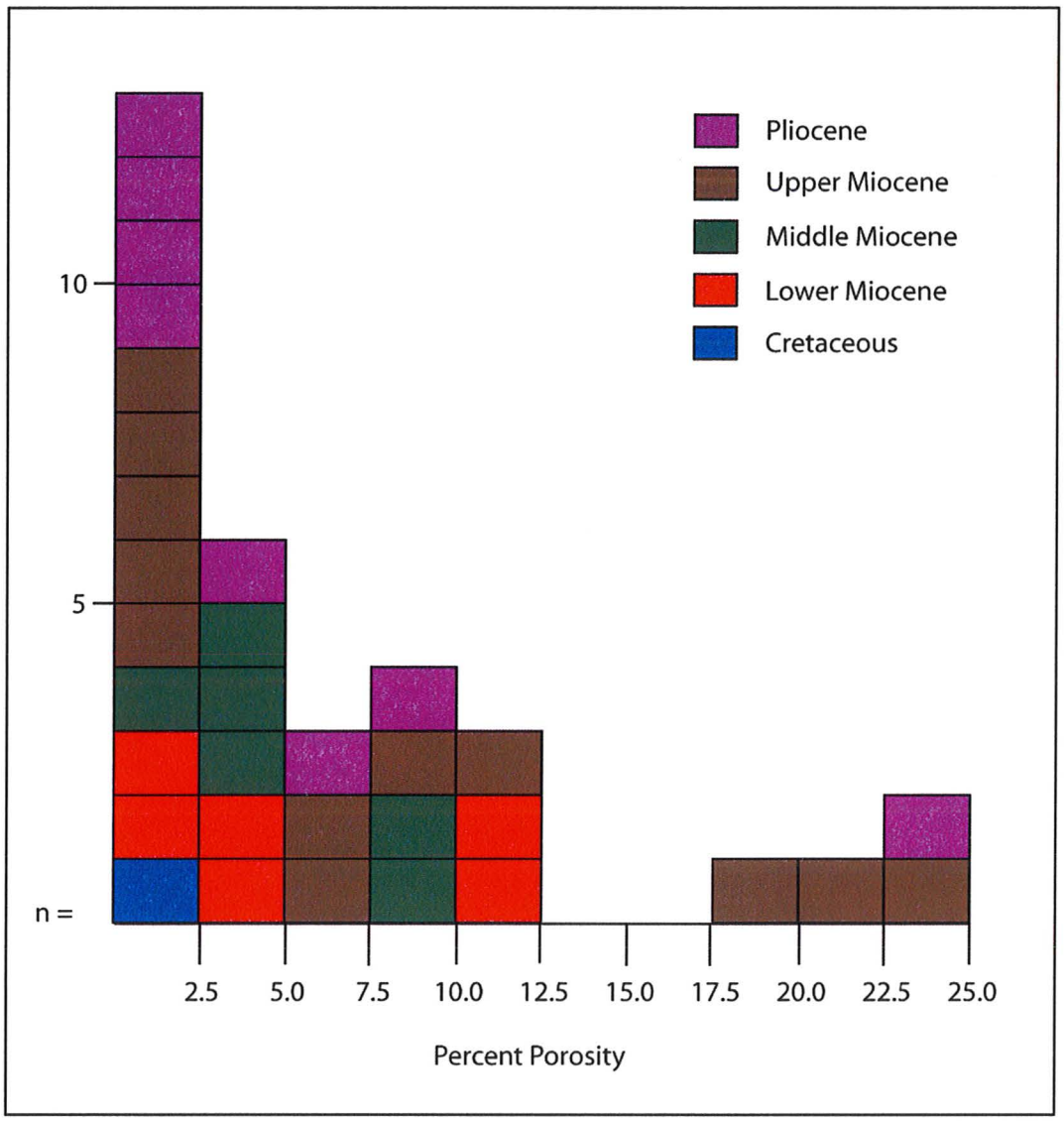
Pliocene
Upper Miocene
Middle Miocene
Lower Miocene
Cretaceous
10
5
n =
2.5
5.0
7.5
10.0
12.5
15.0
17.5
20.0
22.5
25.0
Percent Porosity

FIGURE 15

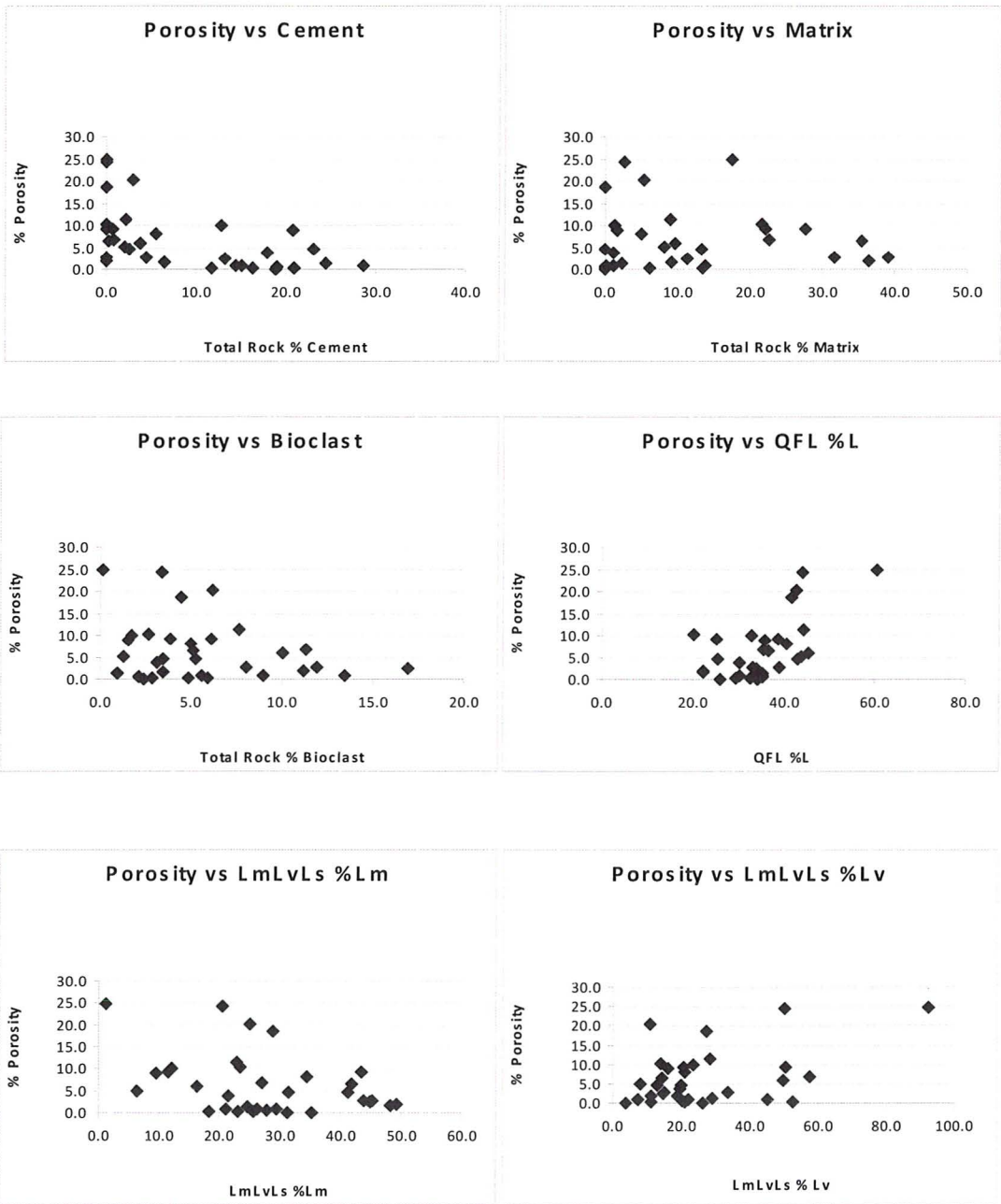
Porosity vs Cement
% Porosity
30.0
25.0
20.0
15.0
10.0
5.0
0.0
0.0
10.0
20.0
30.0
40.0
Total Rock % Cement
Porosity vs Matrix
% Porosity
30.0
25.0
20.0
15.0
10.0
5.0
0.0
0.0
10.0
20.0
30.0
40.0
50.0
Total Rock % Matrix
Porosity vs Bioclast
% Porosity
30.0
25.0
20.0
15.0
10.0
5.0
0.0
0.0
5.0
10.0
15.0
20.0
Total Rock % Bioclast
Porosity vs QFL %L
% Porosity
30.0
25.0
20.0
15.0
10.0
5.0
0.0
0.0
20.0
40.0
60.0
80.0
QFL %L
Porosity vs LmLvLs %Lm
% Porosity
30.0
25.0
20.0
15.0
10.0
5.0
0.0
0.0
10.0
20.0
30.0
40.0
50.0
60.0
LmLvLs %Lm
Porosity vs LmLvLs %Lv
% Porosity
30.0
25.0
20.0
15.0
10.0
5.0
0.0
0.0
20.0
40.0
60.0
80.0
100.0
LmLvLs % Lv

APPENDIX D: MEASURED SECTION DESCRIPTIONS

Section A			
Interval (From base)	**Sample**	**Description**	**Lat/Long Strike, Dip**
0.0 – 0.5 m Base of section	HA1 (0.25 m)	Mudstone: olive gray (5Y 4/1), thinly bedded to massive, moderately hard, moderately weathered, fractured, bioturbated with discrete burrows.	S 38° 41.214 E 177° 38.181 255°, 75°S
0.5 – 30.0 m	HA2 (10.5 m) HA3 (19.0 m)	Interbedded mudstone and sandstone: Mudstone: olive gray (5Y 4/1), thinly bedded to massive, moderately hard, moderately weathered, fractured, bioturbated with discrete burrows. Sandstone: light olive gray (5Y 5/2) to olive gray (5Y 4/1), fine grained, thinly bedded, moderately hard to hard, fractured, bioturbated with discrete burrows.	
30.0 – 60.0 m	HA4 (31.0 m) HA5 (42.0 m) HA6 (52.0 m)	Interbedded mudstone and sandstone: Mudstone: olive gray (5Y 4/1), thinly bedded to massive, moderately hard, moderately weathered, fractured, bioturbated with discrete burrows. Sandstone: light olive gray (5Y 5/2) to olive gray (5Y 4/1), fine grained, thinly bedded, moderately hard to hard, fractured, minor shell fragments, bioturbated with discrete burrows.	249°, 61°S
60.0 – 100.0 m	HA 7 (63.0 m) HA11 (80.0 m) HA10 (91.0 m) HA8 (101.0 m)	Interbedded sandstone and mudstone: Sandstone: light olive gray (5Y 5/2) to olive gray (5Y 4/1), fine grained, thinly bedded, moderately hard to hard, fractured, minor shell fragments, bioturbated with discrete burrows. Mudstone: olive gray (5Y 4/1), thinly bedded to massive, moderately hard, moderately weathered, fractured, bioturbated with discrete burrows.	229°, 48°S
100.0 – 111.0 m Top of section	HA 9 (110.0 m)	Mudstone, olive-gray (5Y 4/1), thinly bedded to massive, moderately hard, moderately weathered, fractured, local burrows	S 38° 41.274 E 177° 38.051

Section B			
Interval (From base)	**Sample**	**Description**	**Lat/Long Strike, Dip**
0.0 – 2.0 m Base of Section	HB1 (1.0 m)	Interbedded mudstone and sandstone: Mudstone: olive gray (5Y 4/1), thinly bedded to massive, moderately hard, moderately weathered, fractured, bioturbated with discrete burrows. Sandstone: light olive gray (5Y 5/2) to olive gray (5Y 4/1), fine grained, thinly bedded, moderately hard to hard, fractured, minor shell fragments, bioturbated with discrete burrows.	S 38° 42.569 E 177° 37.244 275°, 52°S
2.0 – 2.3 m	HB 2	Sandstone concretion: olive gray (5Y 4/1), fine to medium grained, hard, 30 cm thick, minor shell fragments.	
2.3 – 8.0 m	None	Interbedded mudstone and sandstone: Mudstone: olive gray (5Y 4/1), thinly bedded to massive, moderately hard, moderately weathered, fractured, bioturbated with discrete burrows. Sandstone: light olive gray (5Y 5/2) to olive gray (5Y 4/1), fine grained, thinly bedded, moderately hard to hard, fractured, minor shell fragments, bioturbated with discrete burrows.	
8.0 – 12.0 m	None	Covered in vegetation.	
12.0 – 12.5 m	HB3 (12.0 m)	Mudstone: olive gray (5Y 4/1), moderately hard, moderately weathered, bioturbated with discrete burrows.	
12.5 – 19.0 m	None	Covered in vegetation.	
19.0 – 32.5 m	HB5 (22.0 m) HB6 (23.5 m)	Interbedded mudstone and sandstone: Mudstone: olive gray (5Y 4/1), thinly bedded to massive, moderately hard, moderately weathered, fractured, bioturbated with discrete burrows. Sandstone: light olive gray (5Y 5/2) to olive gray (5Y 4/1), fine grained, thinly bedded, moderately hard to hard, fractured, minor shell fragments, bioturbated with discrete burrows.	

Section B (cont) 32.5 – 32.8 m	HB 10	Sandstone concretion, olive gray (5Y 4/1), fine- to medium-grained, hard, 30 cm thick, minor shell fragments	264°, 47°S
32.8 – 88.5 m	HB4 (33.5 m) HB7 (38.0 m) HB8 (43.0 m) HB9 (58.0 m) HB11 (67.0 m)	Interbedded mudstone and sandstone: Mudstone: olive gray (5Y 4/1), thinly bedded to massive, moderately hard, moderately weathered, fractured, bioturbated with discrete burrows. Sandstone: light olive gray (5Y 5/2) to olive gray (5Y 4/1), fine grained, thinly bedded, moderately hard to hard, fractured, minor shell fragments, bioturbated with discrete burrows.	
88.5 – 88.6 m	HB 12	Sandstone: olive gray (5Y 4/1) to dark yellowish orange (10YR 6/6), fine to medium grained, moderately hard, thinly bedded, bioturbated with discrete burrows.	
88.6 – 89.0 m	HB 13	Sandstone concretion: olive gray (5Y 4/1), fine- to medium-grained, hard, minor shell fragments	269°, 50°S
89.0 – 89.1 m	HB 14	Sandstone: olive gray (5Y 4/1) to dusky yellow (5Y 6/4), fine grained, moderately hard, thinly bedded, burrows, minor shell fragments	
89.1 – 132.0 m	HB15 (100 m) HB16 (111 m) HB17 (132 m)	Interbedded mudstone and sandstone: Mudstone: olive gray (5Y 4/1), thinly bedded to massive, moderately hard, moderately weathered, fractured, bioturbated with discrete burrows. Sandstone: light olive gray (5Y 5/2) to olive gray (5Y 4/1), fine grained, thinly bedded, moderately hard to hard, fractured, minor shell fragments, bioturbated with discrete burrows.	277°, 53°S (111 m)
132.0 – 132.5 m	HB 18	Sandstone concretion: olive gray (5Y 4/1), fine- to medium grained, hard, minor shell fragments.	
132.5 – 188.0 m	HB19 (136 m) HB20 (152 m) HB21 (162 m) HB22 (172 m) HB23 (182 m)	Interbedded mudstone and sandstone: Mudstone: olive gray (5Y 4/1), thinly bedded to massive, moderately hard, moderately weathered, fractured, bioturbated with discrete burrows. Sandstone: light olive gray (5Y 5/2) to olive gray (5Y 4/1), fine grained, thinly bedded, moderately hard to hard, fractured, minor shell	

Section B continued		fragments, bioturbated with discrete burrows.	
188.0 – 188.5 m Top of Section	None	Mudstone: olive-gray (5Y 4/1), moderately hard, moderately weathered, local burrows bioturbated with discrete burrows.	S 38° 42.506 E 177° 37.475

Section C			
Interval (From base)	**Sample**	**Description**	**Lat/Long Strike, Dip**
0.0 – 14.0 Base of section	HC1 (3.5 m) HC7 (8.0 m) HC2 (12.0 m)	Interbedded mudstone and sandstone: Mudstone: olive gray (5Y 4/1), thinly bedded to massive, moderately hard, moderately weathered, fractured, bioturbated with discrete burrows. Sandstone: light olive gray (5Y 5/2) to olive gray (5Y 4/1), fine grained, thinly bedded, moderately hard to hard, fractured, minor shell fragments, bioturbated with discrete burrows.	S 38° 43.155 E 177° 36.233 297°, 26°S
14.0 – 14.2 m	HC3 (14.0 m) HC4 (14.1 m)	Mudstone concretion: olive-gray (5Y 4/1), hard, moderately weathered.	
14.2 – 16.5 m	None	Mudstone: olive-gray (5Y 4/1), moderately hard, moderately weathered, minor shell fragments, bioturbated with discrete burrows.	
16.5 – 16.8 m		Mudstone concretion: olive-gray (5Y 4/1), hard, moderately weathered.	
16.8 – 32.0 m	HC5 (17.0 m) HC6 (25.0 m)	Interbedded mudstone and sandstone: Mudstone: olive gray (5Y 4/1), thinly bedded to massive, moderately hard, moderately weathered, fractured, bioturbated with discrete burrows. Sandstone: light olive gray (5Y 5/2) to olive gray (5Y 4/1), fine grained, thinly bedded, moderately hard to hard, fractured, minor shell fragments, bioturbated with discrete burrows.	
32.0 – 70.5 m	None	Section covered in thick vegetation. Estimated thickness 38.5 m. Consists of interbedded mudstone and sandstone as in 16.5 – 32.0 m.	
70.5 – 74.0 m	HC8 (72.0 m)	Fossiliferous wackestone: olive gray (5Y 4/1), hard, poorly sorted (silt to pebble-sized clasts), abundant shell fragments (mm – cm sized), sharp contact with mudstone.	
74.0 – 81.0 m	HC9 (74.0 m) HC10 (80.0 m)	Fossiliferous packstone: dark olive gray, hard, massive, abundant macrofossils at base up to 8 cm long, convex-down, fossils decrease in size and abundance upsection, undulatory contact with wacketstone, increased sand content at 77 m.	
81.0 – 88.0 m	None	Covered	

Section C (continued) 88.0 – 101.0 m	HC11 (90.0 m)	Sandstone: olive gray (5Y 4/1) to dark yellowish orange (10YR 6/6), fine to medium grained, moderately weathered, moderately hard, shell fragments, bioturbated, local concretions, gradational contact with fossiliferous packstone.	
101.0 – 107.5 m	HC12 (101.0 m) HC13 (103.5 m) HC14 (104.5 m) HC15 (105.5 m) HC16 (107.5 m)	Interbedded sandstone and mudstone: Sandstone: olive gray (5Y 4/1), fine to medium grained, moderately weathered, moderately hard, thinly bedded, shell fragments, bioturbated with discrete burrows, local pumice fragments. Mudstone: olive-gray (5Y 4/1), moderately hard, moderately weathered, shell fragments, bioturbated with discrete burrows.	284°, 18°S
		At 107.5 color change in unit from olive gray to alternating orange-brown and light olive gray	
107.5 – 123.0 m	HC17 (108.0 m) HC18 (110.0 m) HC19 (112.0 m) HC20 (113.0 m) HC21 (115.0 m) HC22 (117.0 m) HC23 (119.0 m) HC 25 (122.5 m)	Interbedded sandstone and mudstone: Sandstone: olive gray (5Y 4/1) to dusky yellow (5Y 6/4), fine- to medium grained, moderately weathered, moderately hard, thinly bedded to massive, local shell fragments, bioturbated with discrete burrows. Mudstone, light olive-gray (5Y 6/6) to dusky yellow (5Y 6/4), moderately hard, moderately weathered, minor shell fragments, bioturbated with discrete burrows.	
123.0 – 123.5 m	HC24 (123.2 m)	Sandstone concretion: olive gray (5Y 4/1) to dusky yellow (5Y 6/4), fine- to medium grained, moderately weathered, hard, shell fragments	
123.5 – 125.0 m Top of Section	HC 26 (124.5 m)	Sandstone: olive gray (5Y 4/1) to dark yellowish orange (10YR 6/6), fine to medium grained, moderately weathered, moderately hard, shell fragments,	S 38° 43.144 E 177° 35.865

APPENDIX E: THIN SECTION INDENTIFICATION LIST

Sample # All NZ03-	Age*	Lithology	Location	Stain	Point Count	Comments
HA1	MM	Mudstone	Section A	No	No	
HA2	MM	Mudstone	Section A	No	No	
HA3	MM	Mudstone	Section A	No	No	
HA4	MM	Mudstone	Section A	No	No	
HA5	MM	Mudstone	Section A	Yes	No	Abundant micritic carbonate
HA6	MM	Mudstone	Section A	No	No	
HA7	Middle Miocene	Sandstone	Section A	Yes	Yes	Fine grained, poorly sorted, angular to subrounded grains, carbonate cemented, bioclastic debris
HA8	Middle Miocene	Sandstone	Section A	Yes	Yes	Fine grained, poorly sorted, angular to subrounded grains, carbonate cemented, bioclastic debris
HA9	MM	Mudstone	Section A	No	No	
HA10	Middle Miocene	Sandstone	Section A	Yes	Yes	Fine grained, poorly sorted, angular to subrounded grains, carbonate cemented, bioclastic debris
HA11	Middle Miocene	Sandstone	Section A	Yes	Yes	Fine grained, poorly sorted, angular to subrounded grains, carbonate cemented, bioclastic debris
HAB1	MM	Mudstone	S38° 41.343 E177° 38.031	No	No	Between section A and B
HAB2	Middle Miocene	Sandstone	S38° 41.343 E177° 38.031 Between Section A and B	Yes	Yes	Fine grained, poorly sorted, angular to subrounded grains, straight and concavo-convex grain contacts, bioclastic debris
HAB3	Middle Miocene	Sandstone	S38° 41.569 E177° 37.991 Between Section A and B	Yes	No	Very fine grained, moderately sorted, angular to subrounded grains, carbonate cemented
HAB4	MM	Mudstone	S38° 41.569 E177° 37.991	No	No	Between section A and B
HAB5	Middle Miocene	Sandstone	S38° 42.284 E177° 37.597	Yes	Yes	Fine grained, poorly sorted, angular to subrounded grains, abundant bioclasts, matrix rich

* MM = Middle Miocene, UM = Upper Miocene

APPENDIX E: CONTINUED

Sample # All NZ03-	Age*	Lithology	Location	Stain	Point Count	Comments
HB1	Upper Miocene	Sandstone	Section B	Yes	Yes	Fine grained, poorly sorted, angular to subrounded grains, matrix rich
HB2	Upper Miocene	Sandstone	Section B	Yes	Yes	Fine grained, moderately sorted, angular to subrounded grains, carbonate cemented
HB3	UM	Mudstone	Section B	No	No	
HB4	Upper Miocene	Sandstone	Section B	Yes	Yes	Fine grained, moderately sorted, angular to subrounded grains, carbonate cemented
HB5	UM	Mudstone	Section B	No	No	
HB6	UM	Mudstone	Section B	No	No	
HB7	UM	Mudstone	Section B	No	No	
HB8	UM	Mudstone	Section B	No	No	
HB9	Upper Miocene	Sandstone	Section B	Yes	Yes	Fine grained, moderately sorted, angular to subrounded grains, abundant bioclasts
HB10	Upper Miocene	Sandstone	Section B	Yes	No	Very fine grained, moderately sorted, angular to subrounded grains, carbonate cemented
HB11	Upper Miocene	Sandstone	Section B	Yes	No	Very fine grained, moderately sorted, angular to subrounded grains, matrix rich
HB12	Upper Miocene	Sandstone	Section B	Yes	Yes	Fine to medium grained, moderately sorted, angular to subrounded grains, abundant bioclasts
HB13	Upper Miocene	Sandstone	Section B	Yes	Yes	Fine grained, moderately sorted, angular to subrounded grains, abundant bioclasts, carbonate cemented
HB14	UM	Mudstone	Section B	No	No	
HB15	UM	Mudstone	Section B	No	No	
HB16	UM	Mudstone	Section B	No	No	
HB17	Upper Miocene	Sandstone	Section B	Yes	Yes	Fine grained, moderately sorted, angular to subrounded grains, matrix rich

* MM = Middle Miocene, UM = Upper Miocene

APPENDIX E: CONTINUED

Sample # All NZ03-	Age	Lithology	Location	Stain	Point Count	Comments
HB18	Upper Miocene	Sandstone	Section B	Yes	Yes	Fine grained, moderately sorted, angular to subrounded grains, bioclastic debris, carbonate cemented
HB19	UM	Mudstone	Section B	No	No	
HB20	Upper Miocene	Sandstone	Section B	Yes	Yes	Fine grained, moderately sorted, angular to subrounded grains, porous
HB21	UM	Mudstone	Section B	No	No	
HB22	Upper Miocene	Sandstone	Section B	Yes	Yes	Fine grained, moderately sorted, angular to subrounded grains, matrix rich
HB23	UM	Mudstone	Section B	Yes	No	
HB24	UM	Mudstone	Section B	No	No	
HB30	UM	Mudstone	Section B	No	No	
HC1	Upper Miocene	Sandstone	Section C	Yes	Yes	Medium grained, tuffaceous, poorly to moderately sorted, subangular to subrounded grains
HC2	UM	Mudstone	Section C	No	No	
HB3	UM	Mudstone	Section C	No	No	Micritic carbonate
HC4	UM	Mudstone	Section C	No	No	
HC5	UM	Mudstone	Section C	No	No	
HC6	UM	Mudstone	Section C	No	No	
HC7	UM	Mudstone	Section C	No	No	
HC8	Pliocene	Wackestone	Section C	Yes	No	Medium to coarse grained, poorly sorted, subangular to subrounded grains, abundant bioclastic debris
HC9	Pliocene	Fossiliferous Packstone	Section C	Yes	No	Coarse grained, poorly sorted, subangular to subrounded grains, abundant bioclastic debris, carbonate cemented
HC10	Pliocene	Fossiliferous Packstone	Section C	Yes	No	Coarse grained, poorly sorted, subangular to subrounded grains, abundant bioclastic debris, carbonate cemented

* MM = Middle Miocene, UM = Upper Miocene

APPENDIX E: CONTINUED

Sample # All NZ03-	Age	Lithology	Location	Stain	Point Count	Comments
HC11	Pliocene	Sandstone	Section C	Yes	Yes	Medium grained, poorly sorted, angular to subrounded grains, abundant bioclastic debris, matrix rich
HC12	Pliocene	Mudstone	Section C	Yes	No	
HC13	Pliocene	Sandstone	Section C	Yes	Yes	Very fine to fine grained, poorly sorted, angular to subrounded grains, abundant bioclastic debris, matrix rich
HC14	Pliocene	Sandstone	Section C	Yes	Yes	Fine to medium grained, poorly sorted, angular to subrounded grains, tuffaceous
HC15	Pliocene	Mudstone	Section C	Yes	No	Abundant bioclastic debris
HC16	Pliocene	Sandstone	Section C	Yes	Yes	Very fine to fine grained, poorly sorted, angular to subrounded grains, abundant bioclastic debris
HC17	Pliocene	Sandstone	Section C	Yes	No	Very fine grained, moderately sorted, angular to subrounded grains, bioclastic debris
HC18	Pliocene	Sandstone	Section C	Yes	Yes	Fine to coarse grained, poorly sorted, angular to subrounded grains, abundant bioclasts, carbonate cemented
HC21	Pliocene	Sandstone	Section C	Yes	Yes	Fine grained, moderately sorted, angular to subrounded grains, carbonate cemented
HC22	Pliocene	Sandstone	Section C	No	No	Very fine-grained, moderately sorted, angular to subrounded grains, bioclastic debris
HC24	Pliocene	Sandstone	Section C	Yes	Yes	Fine grained, moderately sorted, angular to subrounded grains, moderate matrix
HC 26	Pliocene	Sandstone	Section C	Yes	Yes	Fine grained, moderately sorted, angular to subrounded grains, carbonate cemented

* MM = Middle Miocene, UM = Upper Miocene

APPENDIX E: CONTINUED

Sample # All NZ03-	Age	Lithology	Location	Stain	Point Count	Comments
201	Lower Miocene	Sandstone	S38° 32.805 E177° 38.806	Yes	Yes	Very fine to fine grained, moderately to poorly, sorted, angular to subrounded grains, carbonate cemented
202	Lower Miocene	Sandstone	S38° 32.805 E177° 38.806	Yes	Yes	Very fine to fine grained, moderately to poorly, sorted, angular to subrounded grains, matrix rich
203	Lower Miocene	Sandstone	S38° 32.647 E177° 37.136	Yes	Yes	Very fine to fine grained, moderately to poorly, sorted, angular to subrounded grains, carbonate cemented, moderate matrix
204	Lower Miocene	Sandstone	S38° 32.647 E177° 37.136	Yes	Yes	Very fine to fine grained, moderately to poorly, sorted, angular to subrounded grains, carbonate cemented, moderate matrix
206	Lower Miocene	Sandstone	S38° 32.290 E177° 36.573	Yes	Yes	Fine grained, moderately to poorly, sorted, angular to subrounded grains, minor cement, moderate matrix
207	Lower Miocene	Mudstone	S38° 32.636 E177° 30.381	No	No	
208	Paleocene	Mudstone	S38° 32.833 E177° 27.080	No	No	Abundant bioclastic debris
210	Oligocene	Mudstone	GPS error	No	No	Abundant bioclastic debris
211	Cretaceous	Sandstone	S38° 32.812 E177° 26.769	Yes	Yes	Fine grained, moderately sorted, angular to subrounded grains, abundant matrix
212	Lower Miocene	Sandstone	S38° 31.807 E177° 32.704	Yes	Yes	Fine grained, poorly to moderately sorted, angular to subrounded grains, moderate matrix

* MM = Middle Miocene, UM = Upper Miocene